2016

Role Of Maternal Sin3a In Reprogramming Gene Expression During Mouse Preimplantation Development

Richard A. Jimenez
University of Pennsylvania, jimenezricharda@gmail.com

Role Of Maternal Sin3a In Reprogramming Gene Expression During Mouse Preimplantation Development

Abstract

In mouse, the maternal-to-zygotic transition entails a dramatic reprogramming of gene expression during the course of zygotic genome activation, which is essential for continued development beyond the 2-cell stage. Superimposed on zygotic genome activation and reprogramming of gene expression is formation of a chromatin-mediated transcriptionally repressive state that promotes repression of genes at the 2-cell stage. Experimentally inducing global histone hyperacetylation relieves this repression and histone deacetylase 1 (HDAC1) is the major HDAC involved in the development of this transcriptionally repressive state. Because SIN3A is essential for mouse development and is part of a HDAC1/2-containing complex, I investigated the role of maternal SIN3A in the development of the global transcriptionally repressive state that develops during the course of genome activation and reprogramming. In addition, previous microarray data generated from our lab of oligo (dT) primed mouse oocyte and 1-cell embryo cDNA revealed an elevation in the relative abundance of the Sin3a transcript between the oocyte and 1-cell stages; the elevation in relative transcript abundance suggests that the Sin3a transcript undergoes translational recruitment during oocyte maturation because the elevation occurs during a period of transcriptional quiescence. Here I show that the Sin3a transcript is recruited for translation during oocyte maturation and following fertilization. I demonstrated that maternal SIN3A is essential for preimplantation development and the reprogramming of genes expression, because inhibiting the maturation-associated increase in SIN3A leads to an arrest in mouse embryonic development and unfaithful reprogramming of gene expression in 2-cell mouse embryos. The mid 1-cell embryo contains the maximum level of maternal SIN3A protein and the protein then rapidly decreases to essentially an undetectable level by the mid 2-cell stage; the rapid loss of maternal SIN3A is likely mediated by the proteasome because a proteasome inhibitor substantially inhibits the loss of maternal SIN3A. Due to the restricted presence of the maturation-associated increase in SIN3A, the function of maternal SIN3A is likely constrained to the 1-cell stage of mouse development. However, the increase in maternal SIN3A does not play a role in the minor ZGA, as depleting maternal SIN3A had no effect on global transcription in 1-cell embryos, but surprisingly results in histone hypoacetylation in 1-cell mouse embryos. Maintaining the presence of maternal SIN3A beyond the 1-cell stage had no effect on pre- and postimplantation development. Collectively, these findings indicate that the maturation-associated increase in SIN3A regulates the reprogramming of gene expression and the oocyte may utilize the translational recruitment of transcripts encoding chromatin-modifying-related factors during oocyte maturation as a post-transcriptional mechanism to faithfully execute the reprogramming of gene expression through the utilization of a maternally-derived transcription machinery.

Degree Type
Dissertation

Degree Name
Doctor of Philosophy (PhD)

Graduate Group
Cell & Molecular Biology

ROLE OF MATERNAL SIN3A IN REPROGRAMMING GENE EXPRESSION DURING MOUSE

PREIMPLANTATION DEVELOPMENT

Richard A. Jiménez

A DISSERTATION

in

Cell and Molecular Biology

Presented to the Faculties of the University of Pennsylvania

in

Partial Fulfillment of the Requirements for the

Degree of Doctor of Philosophy

2016

Supervisor of Dissertation

_____

Richard M. Schultz, Ph.D.

Charles and William L. Day Distinguished Professor of Biology

Graduate Group Chairperson

_____
Daniel S. Kessler, Ph.D.

Associate Professor of Cell and Developmental Biology

Dissertation Committee

Hua-Ying Fan, Ph.D., Assistant Professor of Biochemistry and Biophysics
George L. Gerton, Ph.D., Research Professor of Reproductive Biology in Obstetrics and Gynecology
Peter S. Klein, M.D., Ph.D., Professor of Medicine
Christopher J. Lengner, Ph.D., Assistant Professor of Cell and Developmental Biology

ACKNOWLEGMENTS

ABSTRACT

ROLE OF MATERNAL SIN3A IN REPROGRAMMING GENE EXPRESSION

DURING MOUSE PREIMPLANTATION DEVELOPMENT

Richard A. Jiménez

Richard M. Schultz

In mouse, the maternal-to-zygotic transition entails a dramatic reprogramming of gene expression during the course of zygotic genome activation, which is essential for continued development beyond the 2-cell stage. Superimposed on zygotic genome activation and reprogramming of gene expression is formation of a chromatin-mediated transcriptionally repressive state that promotes repression of genes at the 2-cell stage. Experimentally inducing global histone hyperacetylation relieves this repression and histone deacetylase 1 (HDAC1) is the major HDAC involved in the development of this transcriptionally repressive state. Because SIN3A is essential for mouse development and is part of a HDAC1/2-containing complex, I investigated the role of maternal SIN3A in the development of the global transcriptionally repressive state that develops during the course of genome activation and reprogramming. In addition, previous microarray data generated from our lab of oligo (dT) primed mouse oocyte and 1-cell embryo cDNA revealed an elevation in the relative abundance of the *Sin3a* transcript between the oocyte and 1-cell stages; the elevation in relative transcript abundance suggests that the *Sin3a* transcript undergoes translational recruitment during oocyte maturation because the elevation occurs during a period of transcriptional quiescence. Here I show that the *Sin3a* transcript is recruited for translation during oocyte maturation and following fertilization. I demonstrated that maternal SIN3A is essential for preimplantation development and the reprogramming of genes expression, because inhibiting the maturation-associated increase in SIN3A leads to an arrest in mouse embryonic development and unfaithful reprogramming of gene expression in 2-cell mouse

embryos. The mid 1-cell embryo contains the maximum level of maternal SIN3A protein and the protein then rapidly decreases to essentially an undetectable level by the mid 2-cell stage; the rapid loss of maternal SIN3A is likely mediated by the proteasome because a proteasome inhibitor substantially inhibits the loss of maternal SIN3A. Due to the restricted presence of the maturation-associated increase in SIN3A, the function of maternal SIN3A is likely constrained to the 1-cell stage of mouse development. However, the increase in maternal SIN3A does not play a role in the minor ZGA, as depleting maternal SIN3A had no effect on global transcription in 1-cell embryos, but surprisingly results in histone hypoacetylation in 1-cell mouse embryos. Maintaining the presence of maternal SIN3A beyond the 1-cell stage had no effect on pre- and postimplantation development. Collectively, these findings indicate that the maturation-associated increase in SIN3A regulates the reprogramming of gene expression and the oocyte may utilize the translational recruitment of transcripts encoding chromatin-modifying-related factors during oocyte maturation as a post-transcriptional mechanism to faithfully execute the reprogramming of gene expression through the utilization of a maternally-derived transcription machinery.

TABLE OF CONTENTS

LIST OF ILLUSTRATIONS

LIST OF TABLES

CHAPTER 1: INTRODUCTION

1.1 Overview of mouse oogenesis and preimplantation development

Mammalian oocytes embark on the path to fertilization and embryogenesis within the functional unit of the ovary, the ovarian follicle. Each follicle is composed of a single oocyte arrested in prophase I of meiosis enclosed by one or more layers of specialized somatic cells that communicate with and support the oocyte during its growth and development via gap junctions. Starting with a resting or primordial follicle that comprises of an oocyte surrounded by a single layer of squamous, flattened, pre-granulosa cells, each primordial follicle's prolonged resting phase is interrupted by factors that recruit the follicle for development into a primary follicle. The size of the initial primordial follicle pool in part dictates reproductive senescence in females.

Since the 1950s, the prevailing view was that mammalian females are provided with an extensive, but finite, nonrenewable ovarian reserve around the time of birth for mice or during mid-gestation in humans, which is diminished as the follicles are recruited to grow (Zuckerman, 1951). However, some investigators challenge the 50-year dogma and contend that the ovarian reserve could be replenished by female germline stem cells referred to as oogonial stem cells. These paradigm-shifting studies claim that a population of cells isolated from both neonatal and adult mouse ovaries and adult human ovaries have stem cell characteristics and, specifically for the cells isolated from mouse ovaries, are capable of differentiating into oocytes that are able to mature, ovulate, and fertilize to produce viable embryos and pups (Johnson et al., 2004; Pacchiarotti et al., 2010; Zou et al., 2009; White et al., 2012). The surface protein used to isolate the oogonial stem cells from the ovarian tissue, and the condition of the human ovarian tissues used to isolate the human stem cell-like cells are questionable and need to be investigated more thoroughly in order to definitively determine if the ovarian reserve can be replenished.

The regulatory factors primarily responsible for activation of primordial

follicles are locally produced (Kezele et al., 2002) and include epithelial growth factor kit ligand (KITL), leukemia inhibiting factor (LIF), basic fibroblast growth factor (BFGF), platelet derived growth factor (PDGF), keratinocyte growth factor (KGF) and connective tissue growth factor (CTGF) (Kezele et al., 2005; Nilsson et al., 2006; Nilsson and Skinner, 2004; Skinner, 2005; Schindler et al., 2010). KITL activates the ubiquitous phosphatidylinositol-3-kinase (PI3K) signaling pathway, which is important for the activation and survival of primordial follicles because removal of PTEN, a PI3K antagonist, leads to premature activation of follicles in mouse (Reddy et al., 2008; John et al., 2008). Once the primordial follicle is activated, the surrounding squamous pre-granulosa cells differentiate into cuboidal granulosa cells and begin to proliferate, while the oocyte grows remarkably (increases in size from about 20 μm to 80 μm in diameter) (Eppig and O'Brien, 1996). The growing primary follicles will subsequently develop into secondary and antral follicles.

After exposure to a preovulatory surge of luteinizing hormone (LH) from the pituitary gland, mammalian oocytes overcome meiotic arrest and proceed through meiotic maturation before ovulating (Russell et al., 2007). An increase in the activity of maturation-promoting factor (MPF), a cyclin B-CDK1 complex, drives meiotic progression of mammalian oocytes (Nurse, 1990). Mitogen-activated protein kinase (MAPK) cascade is another important kinase necessary for resumption of meiosis that interacts intimately with the MPF pathway in many species except for mice (Verlhac et al., 1993), where a normal pattern of MPF activity is seen when the MAPK cascade is disrupted in mice lacking c-MOS, a MAPK pathway activator (Araki et al., 1996).

Meiotic maturation entails nuclear membrane breakdown (germinal vesicle breakdown, GVBD), meiosis I spindle assembly, extrusion of the first polar body, and meiosis II spindle assembly. Also, a meiosis-specific deacetylation of histones occurs during meiotic maturation in mouse, where all of the acetylated histones examined, with the exception of H4K8ac, are deacetylated to undetectable levels at the end of meiosis (Kim et al., 2003). Global deacetylation

shortly after meiotic resumption may facilitate chromosome condensation that occurs during oocyte maturation because hyperacetylation of H4K16 likely contributes to defective chromosome condensation observed in *histone deacetylase 2* (*Hdac2*) null mouse oocytes (Ma and Schultz, 2013). Meiotic maturation is complete after arrest at metaphase of meiosis II. Mouse oocytes acquire meiotic competence in a stepwise manner at the time of follicular antrum formation, where they first acquire the ability to reinitiate meiosis but are unable to complete meiosis I and, at a later time, acquire the capacity to complete meiosis I and progress to metaphase of meiosis II (Szybek, 1972; Sorensen and Wassarman, 1976; Wickramasinghe et al., 1991). However, meiotically competent oocytes are unable to support preimplantation embryonic development until additional metabolic and structural modifications are acquired during the periovulatory period (Eppig et al., 1994; Eppig, 1996). Competence to complete preimplantation development is also acquired by growing oocytes in a stepwise manner where they initially acquire the capacity to undergo fertilization and development to the 2-cell stage, and later acquire competence to develop from the 2-cell stage to the blastocyst stage (Eppig and Schroeder, 1989).

After ovulation, the metaphase II arrested mouse egg is fertilized within the oviduct, which triggers the completion of meiosis and formation of a 1-cell embryo. The newly formed 1-cell embryo enters the first mitotic cell cycle that begins with a prolonged Gap 1 (G1) phase during which two spatially separated maternal and paternal haploid pronuclei form, with the larger paternal pronucleus forming first between 4 and 8 hours post-fertilization (hpf) and the maternal pronucleus forming between 5 and 9.5 hpf (Howlett and Bolton, 1985). Each pronucleus undergoes DNA replication before entering the first mitosis to produce a 2-cell embryo, which continues to undergo successive reductive cleavage divisions without a significant increase in cell volume to form the 4-cell embryo, 8-cell embryo, and later the blastocyst (Lehtonen, 1980).

By the late 2-cell stage, the initiation of de novo transcription from the newly formed embryonic genome, known as embryonic genome activation (EGA)

or zygotic gene activation (ZGA), has occurred. ZGA occurs in two phases: (i) minor ZGA occurs at the late one-cell stage, which results in a low-level of global transcriptional activation and generation of non-functional transcripts because they are inefficiently spliced and polyadenylated (Latham et al., 1991; Park et al., 2013; Abe et al., 2015), and (ii) major ZGA occurs at the late two-cell stage, which generates distinct functional transcripts that are not expressed in the germ cells, thus promoting a dramatic reprogramming of gene expression (Zeng et al., 2005; Hamatani et al., 2004). Interestingly, when transcription in mice was analyzed at the 1-cell stage either using a luciferase plasmid-born reporter gene or BrUTP incorporation to assess endogenous gene transcription, enhanced luciferase expression or BrUTP incorporation was observed from the male pronucleus (Ram and Schultz, 1993; Wiekowski et al., 1993; Aoki et al., 1997). This transcription is about four to five times greater in the male pronucleus than that of the female pronucleus, which is consistent with a greater concentration of transcription factors present in the male pronucleus, such as the TATA-box binding protein (TBP) and SP1 transcription factor (Ram and Schultz, 1993; Wiekowski et al., 1993; Worrad et al., 1994). The difference in the transcriptional activity and transcription factor concentration between the male and female pronucleus may likely reflect the difference in chromatin organization between the two pronculei. As discussed below, the male pronucleus exchanges the sperm-derived protamines that densely package the sperm DNA for maternally-derived histones during pronuclear formation (Nonchev and Tsanev, 1990), thereby providing a more open chromatin structure for transcription factors to associate preferentially with and likely enhancing the transcriptional activity of the male pronucleus.

During the 8-cell stage, the first grossly morphological differentiation of the embryo occurs: compaction. Compaction is where the individual blastomeres become nearly indistinguishable due to the formation of desmosomes and gap junctions between the blastomeres (Johnson and Marco, 1986; Fleming et al., 2001). The cell adhesion surface molecule E-cadherin mediates the calcium-

dependent compaction process because E-cadherin null embryos fail to maintain compaction, in addition to failing to form an intact trophectodermal epithelium or a blastocoele cavity (Larue et al., 1994). Following compaction, further cleavage divisions and blastocoele cavity formation, a blastocyst is formed. The blastocyst stage represents the first cellular differentiation event during development where two distinct cellular populations are formed: an outer layer of trophectoderm (TE) cells that give rise to extraembryonic tissues and allow for embryo implantation, and an inner layer of inner cell mass (ICM) cells, which gives rise to the embryo proper. One day after the formation of the blastocyst, the mouse embryo implants into the uterine wall, which marks the completion of preimplantation development.

1.2 Global transcriptional repression and large-scale changes to chromatin structure in mouse oocytes

Towards the end of the oocyte growth phase, a dramatic change in the transcriptional activity and chromatin organization occurs (Bouniol-Bay et al., 1999). Global transcription within the full-grown oocyte rapidly ceases and the oocyte becomes transcriptionally inactive and remains largely inactive until the 2-cell stage is reached in mouse (Moore and Lintern-Moore, 1978). The chromatin in mouse oocytes progressively transforms from a decondensed configuration (referred to as non-surrounded nucleolus, NSN) to a condensed configuration (surrounded nucleolus, SN) during the final stages of oocyte growth (Debey et al., 1993). This alteration in chromatin organization is temporally correlated with but not required for global transcriptional repression in mammalian oocytes because global transcription is repressed in *nucleoplasmin 2* (*Npm2*) null oocytes despite failing to remodel their chromatin into the SN configuration (Bouniol-Bay et al., 1999; Burns et al., 2003; De La Fuente et al., 2004). It has been suggested that the condensed chromatin configuration and silencing of global transcription is not only needed for effective resumption and completion of meiosis by mouse oocytes but is also needed for the subsequent activation of the

5

egg (Liu et al., 2002).

The mechanism responsible for this large-scale chromatin structure alteration and global silencing of transcription in mouse oocytes remains to be determined. However, histone deacetylases (HDACs) may participate in the maintenance of the SN chromatin configuration in mouse oocytes (De La Fuente et al., 2004); exposing transcriptionally quiescent, full-grown mouse oocytes exhibiting the SN configuration to trichostatin A (TSA), an inhibitor of HDACs (Yoshida et al., 1995), induced large-scale chromatin structure decondensation without restoring the transcriptional activity of the oocyte. However, TSA exposure had no effect on the immunostaining patterns of histone H3 and H4 acetylation. The observed failure to restore transcriptional activity in oocytes that underwent chromatin condensation after TSA treatment is consistent with the observation that *Npm2* null mouse oocytes are still able to undergo transcriptional silencing despite failing to undergo chromatin condensation (Burns et al., 2003; De La Fuente et al., 2004).

Changes in the nuclear availability or expression levels of several transcription factors like the TBP and SP1 transcription factor may be responsible for global transcriptional repression in mouse oocytes. Interestingly, the nuclear concentration of both TBP and SP1 decreases during oocyte growth and then increases following fertilization, which is near the time global transcription reinitiates (Worrad et al., 1994). Another locus of regulation may be at the level of the RNA polymerase II holoenzyme itself because a decline in the RNA polymerase II (Pol II) activity was seen as the oocyte reached maximum size (Moore and Lintern-Moore, 1978). In somatic cells, transcription involves a cycle of phosphorylation and dephosphorylation of the carboxy-terminal domain (CTD) of Pol II, specifically the largest subunit RPB1, and therefore may be invovled in global repression of transcription in mouse oocytes (Dahmus, 1996). Several studies have examined the phosphorylation status of RPB1 and found that the CTD of RPB1 undergoes phosphorylation through the action of MAPK during meiotic maturation (Wei et al., 2015; Abe et al., 2010). When the localization of

RPB1 was investigated after permeabilizing the nuclear membrane before fixation, RPB1 was absent from the nuclei of full-grown mouse oocytes, although it remained in the nuclei of growing oocytes.   This suggests that Pol II is dissociated from DNA in full-grown oocytes and may be the cause of global repression of transcription in mouse oocytes. Phosphorylation may destabilize the RNA polymerase II holoenzyme and lead to the dissociation of RNA polymerase II from the DNA. However, how CTD phosphorylation contributes to the abolishment of global transcription in mouse oocytes is not known and needs to be investigated further.

1.3 Zygotic gene activation

ZGA serves two functions for embryonic development. The first function is to replace maternal transcripts with embryonic transcripts that are common to the oocyte and embryo like tubulin (Schultz, 1993; Davis et al., 1996). Expression of these transcripts is essential for further development but does not contribute to the reprogramming of gene expression, although they are part of the gene expression program. The second function of ZGA is to promote a dramatic reprogramming of gene expression by transcribing a new set of mRNAs that are not expressed in the sperm or oocyte. Support for the second function of ZGA was initially shown by analysis of high-resolution, two-dimensional gels, which revealed that a dramatic reprogramming in the pattern of protein expression occurred during the late 1-cell and mid 2-cell stages (Latham et al., 1991). However, only the change in the pattern of protein synthesis that occurred at the 2-cell stage was dependent on de novo RNA transcription because the synthesis of several polypeptides at the 2-cell stage was inhibited by an RNA polymerase II inhibitor (i.e., α-amanitin), whereas the pattern of protein synthesis at the 1-cell stage was unaffected by α-amanitin (Flach et al., 1982; Bolton et al., 1984). Although an observable change in the pattern of protein synthesis by α-amanitin was not seen at the 1-cell stage, it is plausible that proteins affected during 1-cell stage are below the detection limit of the studies' experimental design.

Interestingly, cleavage of 2-cell embryos to the 4-cell stage was inhibited by α-amanitin, whereas cleavage of the 1-cell to 2-cell stage was unaffected (Flach et al., 1982; Bolton et al., 1984). This result suggests that the expression of these new sets of genes at the 2-cell stage is essential for continued development beyond the 2-cell stage because perturbing their expression with an RNA polymerase II inhibitor (i.e., α-amanitin) results in an early embryonic arrest. The reprogramming process is likely essential for transforming a highly differentiated oocyte and sperm into a totipotent blastomere, and if this crucial step is not successfully performed, it is plausible that a developmental checkpoint prevents further development of the embryo.

1.4 Transcriptionally repressive state

Superimposed on zygotic genome activation (ZGA) is the development of a transcriptionally repressive state. Several lines of evidence support the developmental acquisition of a repressive state in the 2-cell embryo. Studies using luciferase plasmid-born reporter genes driven by the thymidine kinase (tk)-promoter demonstrated that by the 2-cell stage efficient luciferase expression requires an enhancer, e.g., the embryo-responsive polyomavirus F101 enhancer (Wiekowski et al., 1991; Majumder et al., 1993). Enhancers are regulatory DNA elements that confer transcriptional activation by recruiting RNA polymerase, histone modifying enzymes or chromatin remodelers to promoters in a distance- and orientation- independent manner (Johnson and Bresnick, 2002). The requirement for an enhancer following genome activation during the 2-cell stage suggests formation of a transcriptionally repressive state that is relieved by an enhancer. Moreover, the strength of the transcriptionally repressive state increases with development because the level of enhancer-mediated stimulation of luciferase expression increased as 2-cell embryos developed into 4-cell embryos (Henery et al., 1995). Establishment of this repressive state involves DNA replication; inhibiting the second round of DNA replication with aphidicolin relieves the requirement for an enhancer for efficient transcription (Wiekowski et

al., 1991; Henery et al., 1995).

Inducing histone acetylation by treating mouse embryos with butyrate, which is another inhibitor of histone deacetylases, also relieves the repression in 2-cell embryos. Histone hyperacetylation lead to an 18-fold stimulation of a promoter lacking an enhancer and reduced the enhancer stimulation of a promoter to only 2-fold in 2-cell embryos (Wiekowski et al., 1991). Experimentally induced histone hyperacetylation also relieves the repression observed for the expression of endogenous genes that transiently increases between the 1-cell and mid 2-cell stage, and then decreases by the late 2-cell/4-cell stage. A normal decrease in expression of endogenous genes like *Eif1a* is seen with formation of the transcriptionally repressive state, which is prevented when histone hyperacetylation is induced (Davis et al., 1996). The repression of endogenous genes is believed to be global because inducing histone hyperacetylation results in a 2-fold increase in the extent of global BrUTP incorporation during the 2-cell stage (Aoki et al., 1997). The increase in the total amount of BrUTP in the presence of a histone deacetylase inhibitor indicates an increase in global transcription due to a global relief of transcriptional repression. Therefore, formation of an enhancer and histone hyperacetylation responsive transcriptionally repressive state by the 2-cell stage of development is likely mediated by changes in histone acetylation and thus global changes in chromatin structure.

Histone hyperacetylation also inhibited development of mouse embryos beyond the 2-cell stage. Experimentally inducing histone hyperacetylation in 2-cell embryos using TSA prevented cleavage to the 4-cell stage, whereas treatment of 1-cell embryos with TSA did not inhibit cleavage to the 2-cell stage (Ma et al., 2001). Formation of the chromatin-mediated transcriptionally repressive state may be essential for further development because relief of this repressive state by inducing histone hyperacetylation prevents cleavage of 2-cell embryos. Histone deacetylase 1 (HDAC1) is the major HDAC involved in the development of this transcriptionally repressive state. Knockdown of HDAC1, but

not HDAC2 in preimplantation embryos leads to hyperacetylation of histone H4 and prevented the normal decrease in expression of some endogenous genes including *Eif1a* (Ma and Schultz, 2008). These results are consistent with the results observed following treatment of embryos with TSA. However, induction of histone hyperacetylation following depletion of HDAC1 in 2-cell embryos did not stimulate global transcription as observed following treatment with TSA. A likely explanation for this difference is that TSA treatment induces a more profound increase in histone acetylation than that observed following depletion of HDAC1.

The role of the transcriptionally repressive state during the 2-cell stage of development needs to be further investigated. It is likely that the development of the repressive stage is needed to sculpt and refine the global ZGA process that is occurring at around the same time that the repressive state is formed. A foreseen consequence of a global process such as ZGA may be the inappropriate expression of many genes that are not conducive to the continued development of the embryo. Formation of a transcriptionally repressive state may decrease or terminate expression of the inappropriately activated genes, but allow the continued expression of genes that are regulated by strong promoters or enhancers that are able to relieve the newly formed transcriptionally repressive state.

1.5 Epigenetic reprograming in the zygote

Chromatin organization and epigenetic modifications of the male and female genomes are distinct at fertilization. The male and female genomes are also in different stages of the cell cycle at insemination; the male genome has completed meiosis, whereas the female genome is arrested at metaphase II and needs to complete the second meiotic division. Two different types of epigenetic modifications occur during zygotic development. One type occurs at the chromatin level, whereas the other occurs at the DNA methylation level. Upon fertilization, but before the first round of DNA replication, the unique, highly condensed protamine-rich chromatin of the sperm changes dramatically; the

protamines are rapidly exchanged with maternally-derived histones, whereas the maternal genome essentially retains a chromatin structure present at fertilization (Nonchev and Tsanev, 1990). The exchange and assembly of the new nucleosomes on the paternal genome requires histone chaperones. Specifically, histone variant H3.3-containing nucleosomes are assembled onto the sperm DNA and this process requires the H3.3-specific histone chaperone protein HIRA. Loss of maternal HIRA in mouse zygotes leads to a paternal genome devoid of acetylated-H4, H2A and H3.3 (Lin et al., 2014; Loppin et al., 2005).

Histone replacement on the paternal genome affords the newly formed embryo a unique window of opportunity to dramatically remodel its chromatin. Once the histones are assembled and incorporated into the nucleosomes, changes in the acetylation and methylation pattern can occur. Histones of both the maternal and paternal genome become acetylated soon after fertilization, with the paternal chromatin appearing more acetylated when compared to the maternal chromatin (Adenot et al., 1997; Santos et al., 2002). Soon after histone acquisition of the paternal genome, the methylation status of the histones in the newly assembled nucleosomes changes also. The paternal chromatin initially lacks H3K4me1 and H3K4me3 (active marks), H3K9me1, H3K9me2 and H3K9me3, H3K27me1, H3K27me2 and H3K27me3, and H4K20me3 (repressive marks), whereas the maternal genome maintains all of these histone modifications. However, the paternal chromatin gains new histone post-translational modifications such as H3K9me1 and H3K27me1 immediately after the protamine-histone exchange (Santos et al., 2005), and gains H3K4me1 and H3K4me3, H3K9me2, H3K27me2 and H3K27me3 modifications later during pronuclear development (Erhardt et al., 2003; Lepikhov and Walter, 2004; Liu et al., 2004). The de novo appearance of histone methylation modifications within the paternal pronucleus at histone residues that can sustain alternative histone modifications indicates that a rapid deacetylation and subsequent monomethylation process by histone deacetylases and monomethyltransferases has occurred at these sites. SET 7/9 methyltransferases are needed for K3K4

monomethylation, G9a and ESET methyltransferases are needed for K3K9me1, and the monomethyltransferases, EZH1/EED and EZH2/EED are responsible for H3K27me1 (Wang et al., 2001; Tachibana et al., 2002; Shen et al., 2008). The new histone modifications accumulating in the paternal pronucleus conceivably shapes the newly formed paternal chromatin to a state equivalent to the mature maternal chromatin.

At the time of fertilization, the epigenetic modifications at the DNA level are diverse and change dramatically during zygotic development. The two genomes contain sex-specific 5-methlycytosine (5mC) patterns, which are acquired during development of the gametes. The global DNA methylation level in the paternal haploid genome is high, with 80%-90% of all CpG dinucleotides being methylated (Mayer et al., 2000; Santos et al., 2002; Peat et al., 2014). The female haploid genome is less heavily methylated in the oocyte, where about 40% of all CpG dinucleotides are methylated (Howlett and Reik, 1991; Smallwood et al., 2011; Peat et al., 2014). Interestingly, over a decade ago, two pivotal studies observed by different methods that fertilization triggers rapid global and active loss of DNA methylation within the paternal genome, but not its maternal counterpart (Mayer et al., 2000; Oswald et al., 2000). The initiation of this active DNA demethylation occurs shortly after histone acquisition of the paternal genome as evaluated by indirect immunofluorescence (Mayer et al., 2000; Dean et al., 2001; Santos et al., 2002; Beaujean et al., 2004; Fulka et al., 2004) and by bisulphite sequencing at specific loci (Oswald et al., 2000; Lane et al., 2003).

Recently, a vital enzyme responsible for mediating active DNA demethylation during preimplantation development was discovered to be TET3 (Iqbal et al., 2011; Gu et al., 2011; Wossidlo et al., 2011). TET3 asymmetrically localizes to the paternal pronucleus and is absent from the female pronucleus potentially due to inhibition by PGC7/Stella binding to the H3K9me2 enriched maternal genome (Gu et al., 2011; Nakamura et al., 2012). TET3 is part of the Ten-eleven translocation (TET) family of dioxygenases that includes TET1 and

TET2 (Ito et al., 2010, Thiliani et al., 2009). TET3 mediates the oxidation of the paternal 5mC to 5-hydroxymethylcytosine (5hmC), 5-formylcytosine (5fC) and 5-carboxylcytosine (5caC), which are gradually lost during each successive reductive cleavage division along with the maternal 5mC (Inoue et al., 2011; Inoue and Zhang, 2011; Rougier et al., 1998). Deletion of maternal TET3 leads to a retention of 5mC in the paternal pronucleus and reduced fecundity (Gu et al., 2011). It is unclear what role the demethylation process has on development of the embryo, but the erasure of the specialized germ cell epigenetic memory may be essential to generate a clean, baseline state on which to build upon to create a new DNA landscape for the viability of the embryo since perturbing one of the demehtylation mechanisms leads to a reduction of embryo viability.

1.6 SIN3A-co-represssor complex and HDAC1/2-containing complexes

The SIN3A co-repressor complex, composed of SWI-independent-3 homolog A (SIN3A), histone deacetylase 1/2 (HDAC1/2), suppressor of defective silencing protein 3 (SDS3), retinoblastoma binding protein 4/7 (RBBP4/7), SIN3A-associated protein 30/130/180 (SAP30/130/180), SIN3A associated protein 18 (SAP18), retinoblastoma-binding protein 1 (RBP1), inhibitor of growth family, member 1/2 (ING1/2), breast cancer metastasis suppressor 1 (BRMS1), family with sequence similarity 60, member A (FAM60A), PHD finger protein 12 (PHF12), and mortality factor 4 like 1 (MORF4L1), interacts with transcription factors like TP53, SOX2, E2F4 and Krüppel-like factor 11 (KLF11) (Smith et al., 2012; Kadamb et al., 2013; Bansal et al., 2015). With no enzymatic or recognizable DNA-binding activity, the highly conserved SIN3A protein acts as a scaffold upon which a diverse set of proteins dock (Silverstein and Ekwall, 2005). This scaffolding role of SIN3A makes it an essential component of the multi-subunit SIN3A co-repressor complex that has been described in many organisms from plants to humans (Hill et al., 2008; Hassig et al., 1997). Due to its scaffolding function, SIN3A allows for transcription factors and various chromatin remodelers to be in close proximity of one another to target and reorganize the

chromatin. The SIN3A co-repressor complex is recruited to promoters of several genes via transcription factors resulting in localized histone deacetylation and gene silencing (Ayer et al., 1995; Kadosh and Struhl, 1997; Knoepfler and Eisenman, 1999). Although the SIN3A co-repressor complex can extend its enzymatic function by interacting with other enzymes such as the ESET histone methyltransferase (Yang et al., 2003), the complex is commonly referred to as a co-repressor complex primarily due to its HDAC activity that leads to transcriptional repression (Bansal et al., 2016).

Interestingly, SIN3A is now being appreciated as a dual regulator of transcription because SIN3A both activates and represses transcription.   For example, in mouse embryonic stem (ES) cells, *Sin3a* stimulates *Nanog* expression though SOX2 under proliferating conditions (Baltus et al., 2009a). However, at the same locus, when TP53 recruits SIN3A to the *Nanog* promoter during mouse ES cell differentiation, expression of *Nanog* is suppressed (Lin et al., 2005). These studies suggest that the SIN3A-co-repressor complex may differentially regulate a common set of SIN3A target genes depending on the cellular state (i.e. a proliferative or differentiative state). However, the molecular mechanisms explaining SIN3A mediated gene activation is so far unknown. Whether the mechanism is HDAC-dependent or independent is not known. At the *Nanog* locus, there is evidence that activation of transcription may be HDAC-dependent, but the target of the HDAC activity may not involve histones but rather the transcription factor SOX2. Because the nuclear export and proteasomal degradation of SOX2 is mediated by acetylation in mouse ES cells (Baltus et al., 2009b), it is conceivable that the SIN3A-HDAC complex maintains SOX2 in the deacetylated state in order to retain SOX2 in the nucleus and sustain the expression of *Nanog*.

The SIN3A co-repressor complex is not the sole HDAC1/2-containing complex. Several other HDAC1/2-containing complexes other than the SIN3A co-repressor have been characterized in mammals. These include the nucleosome remodeling and deacetylase (NuRD) complex (Denslow and Wade,

2007), the ES cell specific NANOG and Oct4 (POU5F1) associated deacetylase (NODE) complex (Liang et al., 2008), the CoREST complex (You et al., 2001), and the SHIP1 containing complex, which is a testis-specific complex (Choi et al., 2008). HDAC1/2 are present in large multiprotein complexes mainly because HDAC1/2 do not bind DNA directly and are likely inactive when they not incorporated into a complex. The necessity of HDAC1/2 to be integrated into a complex in order to function was shown for the NuRD complex. In the absence of MTA2, an interacting member of the NuRD complex, the HDAC enzymatic activity of the complex was severely compromised (Zhang et al., 1999). This finding suggests that MTA2 may promote the formation of the catalytic active histone deacetylase center of the NuRD complex.

With the involvement of HDACs in the establishment of the transcriptionally repressive state during early embryonic development and the existence of several HDAC-containing complexes, there is clearly an emerging question as to which HDAC-containing complex is mediating the development of the repressive state. This question can be addressed, in part, by assessing each HDAC-containing complexes' role in early development and the formation of the repressive state.

The following work focuses on the SIN3A-co-repressor complex because SIN3A is essential for mouse development. In this system, zygotic *Sin3a* deletion leads to embryonic lethality shortly after implantation (around Embryonic Day 6.5) (Cowley et al., 2005; Dannenberg et al., 2005). Because crossing *Sin3a* heterozygous mice generated the *Sin3a* null embryos, the experimental design limited the scope of their observations to zygotic SIN3A and did not address the role of maternal SIN3A, specifically, the role of SIN3A in the development of the transcriptionally repressive state.

To investigate the role of maternal SIN3A in the development of the repressive state during mouse preimplantation development, I utilized a combined morpholino/small interfering RNA (siRNA) approach to deplete embryos of maternal SIN3A. This allowed me to assay the contributions of

maternal SIN3A in a live embryo, and to determine if maternal SIN3A is essential prior to Embryonic Day 6.5. Because SIN3A has been strongly associated with the transcriptional regulation of several genes, specifically gene repression, I hypothesized that depleting mouse embryos of maternal SIN3A would result in a failure to form the transcriptional repressive state, thereby, affecting the fidelity of the reprogramming of gene expression during the two-cell stage of mouse embryonic development. In Chapter 3, I describe our efforts to characterize the role of maternal SIN3A in the formation of the transcriptionally repressive state. I show that maternal SIN3A is encoded by a dormant maternal mRNA that is translationally recruited during oocyte maturation and following fertilization. I also describe the consequences of inhibiting the maturation-associated increase in SIN3A in mouse embryos.

CHAPTER 2: MATERIALS AND METHODS

Oocyte and Embryo Collection, and Embryo Culture and Transfer

Germinal vesicle (GV)-intact oocytes were collected from 6-week-old CF-1 female mice that received an intraperitoneal (IP) injection of 5 IU pregnant mare serum gonadotropin (eCG, Sigma). Following 44 h of eCG injection, the mice were killed by CO_2 asphyxiation, the ovaries excised and placed in collection medium. The collection medium used was minimal essential medium (Earle's salts) containing gentamicin (10 ug/mL), polyvinylpyrrolidone (3 mg/mL), pyruvate (100 ug/mL), and 10 mM Hepes, pH 7.21 (MEM/PVP). 10 uM milrinone was present in the collection medium to maintain meiotic arrest (Tsafriri et al., 1996). After puncturing the ovaries with 30.5-gauge needles, large preovulatory follicles were released and collected. The cumulus cells were gently stripped from cumulus-cell enclosed oocytes (CEOs) using a mouth-operated pipette (Schultz et al., 1983). Metaphase I (MI) oocytes were collected 7 h after transferring full-grown oocytes to milrinone-free Chatot Ziomek Brinster (CZB) medium (Chatot et al., 1989). In vivo metaphase II (MII) eggs were collected from eCG-primed 6-week old CF-1 female mice 13-16 h following hCG administration as previously described (Endo et al., 1987). In brief, superovulated female mice were given an IP injection of 5 IU of eCG, followed 48 h later by 5 IU human chorionic gonadotropin (hCG, Sigma). The superovulated mice were killed by CO_2 asphyxiation 13-16 h after hCG injection, the oviducts excised, and the eggs obtained by tearing the oviducts with 27.5-gauge needles in MEM/PVP containing 3 mg/mL hyaluronidase (Sigma). As soon as the cumulus cells detach from the eggs, the eggs were washed in several drops of MEM/PVP. In vitro MII eggs were also obtained following maturation in vitro for 16-18 h after transferring full-grown oocytes to milrinone-free CZB medium. Mid 1-cell, late 1-cell, early 2-cell, mid 2-cell, 8-cell and blastocyst stage embryos were collected from eCG-primed 6-week old CF-1 female mice mated to B6D2F1/J males (Jackson Laboratory) by flushing either the oviduct or uterus 20-

21, 30-32, 36, 44, 68, 94-96 h post hCG as previously described (Manejwala et al., 1986). The superovulated females were placed overnight in a cage with a single male and examined for the presence of a vaginal plug the next morning.

For the mouse embryo transfer experiments, $Gfp^{-/-}$ virgin CF-1 female mice were mated to $Gfp^{+/-}$ males. The resulting $Gfp^{+/-}$ embryos were collected 18 h after fertilization, and embryos with two distinct pronuclei were microinjected at 19–21 h after fertilization with T7 C-terminal-tagged $Sin3a$ cRNA; controls were injected with buffer. The embryos were cultured for 96 h (to E4.5) in KSOM medium as described above at which time the number of blastocysts was scored and GFP expression assessed. To determine the incidence of implantation of $Sin3a$ cRNA-injected embryos compared with control embryos, blastocyst stage embryos were transferred to pseudopregnant female mice on Postcoital Day 3.5 using the Non-Surgical Embryo Transfer Device (Paratechs) according to the manufacturer's protocol. Each female received 8-10 embryos, half of which were injected with $Sin3a$ ($Gfp^{-/-}$ or $Gfp^{+/-}$) and the other half injected with buffer ($Gfp^{+/-}$ or $Gfp^{-/-}$) to serve as controls. Thus, each female received 4-5 GFP-positive (or negative) $Sin3a$ cRNA-injected embryos and 4-5 GFP-negative (or positive) control embryos. The females were killed by CO_2 asphyxiation 7 days after embryo transfer (E10.5), and the presence of GFP expression in the implanted embryos was assessed.

All animal experiments were approved by the Institutional Animal Use and Care Committee and were consistent with the National Institutes of Health guidelines.

Microinjection

Full-grown GV-intact oocytes isolated from CEOs were microinjected with 5 pl of a solution containing 5 μM short interfering RNA (siRNA) and 1 mM morpholino while being cultured in MEM supplemented with 10 uM milrinone and 20% fetal bovine serum (Kurasawa et al., 1989). The cRNA for $Sin3a$-T7 and GFP were injected at 580 ng/μl. The $Sin3a$ (s73784, Ambion) and control

Luciferase siRNA (D-001100-01-05, Dharmacon) were both injected at a concentration of 5 μM. The concentration of the *Sin3a* (5'-CCTGGTCATCCAAACGTCGCTTCAT-3', Gene Tools) and standard control morpholinos (Gene Tools) was 1 mM.

IVM and IVF

For in vitro maturation (IVM) and in vitro fertilization (IVF), CEOs from 24-day-old B6SJLF1/J females primed with eCG for 44 h before isolation were collected in MEM supplemented with 10 uM milrinone and 20% fetal bovine serum as previously described (Downs et al., 1986). The cumulus cells were gently stripped from the CEOs using a mouth-operated pipette. The medium used for oocyte maturation was MEM supplemented with 0.23 mM pyruvate and 20% fetal bovine serum without milrinone and FSH. The denuded oocytes were cultured in this medium under drops of mineral oil at 37 °C in 5% O_2, 5% CO_2 and 90% N_2 for 13 -14 h in the presence of 10-15 CEOs as previously described (Schroeder and Eppig, 1984).

Fertilization of eggs in vitro was performed as previously described (Hoppe & Pitts, 1973; Schroeder and Eppig, 1984). Sperm suspensions were obtained from the cauda epididymis of B6SJL males that were at least 4 months old, and housed individually for at least 3 days. The cauda epididymis were excised and minced into 0.9 mL of warm equilibrated TYH fertilization medium supplemented with 4 mg/mL of BSA (Toyoda et al., 1971; Tateno and Kamiguchi, 2007) overlaid with mineral oil. The sperm were allowed to disperse from the minced epididymis for 5-10 min. The suspension was examined qualitatively for vigor, and a dilute sample was used to quantify the sperm concentration using a hemocytometer. The in vitro MII eggs were washed in 4 drops of fertilization medium and placed into 50 μl drops overlaid with mineral oil. The in vitro MII eggs were then inseminated using capacitated sperm (5 x 10^5 sperm/mL) capacitated for 1.5 h at 37 °C in 5% O_2, 5% CO_2 and 90% N_2. After 3 h of incubation, the sperm adhering to the eggs were removed using a fine-bore

19

mouth-operated pipette, and the inseminated eggs were then transferred to and cultured in KSOM medium (Erbach et al., 1994; Ho et al., 1995) under mineral oil at 37°C in 5% O_2, 5% CO_2 and 90% N_2.

Synchronization of 1-cell and 2-cell Embryos

One-cell embryos generated from IVF were cultured in KSOM medium and examined for the appearance of pronuclei at 1 h intervals starting at 3 h post-insemination or following the first cleavage at 2 h intervals starting at 19 h post-insemination. Embryos that formed pronuclei or underwent the first cleavage within the previous hour were collected and cultured separately. One-cell embryos used for global histone modification immunofluorescence analysis were fixed 6 h after pronucleus formation. One-cell or 2-cell embryos used for global transcriptional analysis were added to 2 mM 5-ethynyl uridine (EU) in KSOM medium from the time the first pronucleus formed until 17 h post-insemination or 12 h post-cleavage for 1 h. Two-cell embryos used for microarray analysis were collected and frozen 12 h post-cleavage.

Immunofluorescence

Oocyte, MI, egg, or embryo samples were all collected and fixed in 2.5% paraformaldehyde for 20 min at room temperature within 2 days. The samples were permeabilized for 15 min in PBS containing 0.1% Triton X-100, washed and blocked for 30 min with PBS containing 0.1% BSA, 0.01% Tween-20 at room temperature. Then the cells were incubated with the SIN3A primary antibody (MBL International) at 1:100 in blocking buffer overnight at 4 °C, followed by three 15-min washes in blocking solution. After the washes, the samples were incubated for 1 h with the anti-rabbit cy5-conjugated secondary antibody (Jackson ImmunoResearch) diluted 1:100 in blocking solution.

In some experiments, 1-cell embryos were first permeabilized for 15 min in PBS containing 0.1% Triton X-100, washed and then fixed in 2.5% paraformaldehyde for 20 min at room temperature. The samples were then

processed as described above.

Polyclonal antibodies against histone H3 acetylated on K18 (39756, Active Motif, 1:100), histone H4 acetylated on K5 (06-759, Millipore, 1:50), histone H4 acetylated on K8 (06-760, Millipore, 1:100), histone H4 acetylated on K12 (06-761, Millipore, 1:100), histone H4 acetylated on K16 (06-762, Millipore, 1:100) were used to assess histone modifications. Trichostatin A (TSA, Sigma), a histone deacetylase inhibitor, was used to induce histone hyperacetylation of early 1-cell embryos by treating the cells with 50 nM TSA for 5 h. Polyclonal antibody against NANOG (ab80892, Abcam, 1:200), and monoclonal antibodies against POU5F1/OCT4 (sc-5279, Santa Cruz Biotechnology, 1:100) and CDX2 (MU392A-UC, BioGenex, 1:100) were used to assess these proteins in the blastocyst. After three 15-min washes with blocking solution, the samples were incubated with 1 μM SYTOX Green (Molecular Probes) to stain DNA. The cells were mounted under a coverslip in VECTASHIELD medium (Vector Laboratories). A Leica TCS SP laser-scanning confocal microscope captured the images and detected the fluorescence intensity of the samples. For each experiment, all samples were processed in parallel. For SIN3A, the laser power was adjusted so that the signal intensity was below saturation for the developmental stage that showed the highest signal intensity and all images were then scanned at that laser power. With all the images being scanned at the same laser power in a developmental series, the signal intensity for SIN3A can be compared to different developmental stages. The images were processed and the fluorescence intensity was quantified using ImageJ software (National Institutes of Health).

Immunoblot Analysis

Protein samples from 40 oocyte, eggs or embryos were solubilized in Laemmli sample buffer (Laemmli and Quittner, 1974), resolved by SDS-PAGE (7.5% gel) and transferred to a PVDF membrane. The membrane was blocked in 2% Amersham ECL prime blocking reagent (GE Healthcare Life Sciences) for

1 h and incubated at 4 °C overnight with the primary antibody in blocking solution. The membrane was then washed four times with PBST (phosphate-buffered saline with 0.1% Tween-20), incubated with a secondary antibody conjugated with horseradish peroxidase for 1 h in blocking solution and washed four times with PBST. The signal was detected with the Amersham ECL Select Western blotting detection reagent (GE Healthcare Life Sciences) according to the manufacturer's instructions. The rabbit SIN3A primary antibody (BMP004, MBL International) was diluted 1:2,000 in blocking solution. The TUBA primary antibody (T6074, Sigma) was diluted 1:5,000 in blocking solution. The Amersham ECL secondary antibody (NA934V and NA931V, GE Healthcare Life Sciences) was diluted 1:75,000 in blocking solution.

Proteasome Inhibition

Mid 1-cell embryos were collected as described above and cultured in KSOM medium containing either 20 μM MG132 (Sigma), a reversible proteasome inhibitor (Palombella et al., 1994), or DMSO (Sigma) at 37 °C in 5% O_2, 5% CO_2 and 90% N_2. After 5 and 10 h of culture, 40 1-cell embryos were collected from the MG132 group and the DMSO control group at each of the two time points for immunoblot analysis.

RNA Extraction, RT-PCR and Real-Time PCR

Total RNA from 20 embryos was extracted using the Arcturus PicoPure RNA Isolation Kit (Life Technologies) according to the manufacturer's instructions. However, before the cell extract was added to the purification column, *Gfp* cRNA was added to the samples as an external standard. Reverse transcription reactions were performed using Superscript II reverse transcriptase (Invitrogen) and random hexamers in a 20 ul reaction volume (Ma and Schultz, 2008). The cDNA was then quantified by quantitative real-time PCR (qRT-PCR) using the ABI Taqman Assay-on-demand probe/primer sets for *Sin3a* and *GFP* as previously described (Zeng et al., 2004). For each qRT-PCR, one embryo

equivalent of cDNA was used with a minimum of three replicates as well as a minus RT and minus template control. Quantification was normalized to GFP.

DNA Replication Assay by BrdUTP Incorporation

Inseminated MII eggs were cultured in KSOM containing 10 μM BrdUTP either 3 h post-insemination or soon after the first cleavage. One-cell embryos were fixed 19 h post-insemination and the 2-cell embryos were fixed 34 h post-insemination. The embryos were then processed using the immunofluorescence protocol described above with the addition of a denaturing step and neutralizing step after permeabilization. The samples were denatured for 30 min in 2N HCl and neutralized for 20 min in 100 mM Tris-HCl, pH 8.5 at room temperature. The samples were incubated with the mouse monoclonal anti-BrdUTP antibody (11170376001, Roche) at 1:50 in blocking solution overnight at 4 °C. The samples were incubated with the secondary FITC anti-mouse IgG1 antibody (1144-02, Southern Biotech) at 1:100 in blocking solution for 1 h. The samples were mounted in VECTASHIELD medium (Vector Laboratories) containing 2 μM TO-PRO-3 (Life Technologies).

Global Transcriptional Assay

Click-iT RNA Imaging kit (Invitrogen) was used to assay global transcription following the manufacturer's instructions. Briefly, synchronized 2-cell embryos were cultured with 2 mM 5-ethynyl uridine (EU) in KSOM medium for 1 h before fixation in 2.5% paraformaldehyde for 20 min at room temperature. To assay global transcription in 1-cell embryos, the synchronized embryos were incubated in KSOM medium containing 2 mM EU from the time the first pronucleus formed until 17 h post-insemination. After washing and membrane permeabilization, incorporated EU was detected using the Click-iT detection molecule. The samples were mounted in VECTASHIELD medium (Vector Laboratories) containing 2 μM TO-PRO-3 (Life Technologies) to visualize the DNA. DNA and EU were visualized using a Leica TCS SP laser-scanning

confocal microscopy. The intensity of the fluorescence was quantified using ImageJ software (National Institutes of Health) as previously described (Aoki et al., 1997).

Plasmid DNA Constructs

To generate a T7 C-terminal-tagged *Sin3a* cRNA, mouse *Sin3a* coding sequence was amplified from mouse cDNA clone 6837144 (Thermo Scientific Open Biosystems) by PCR using the forward primer 5'-gaggGCATGCcATGAAGaGgaGacTGGAcGACCA -3' and the reverse primer 5'-gcgGTCGACCCGGCCACGCGTAGGGGCTTTGAATACTGTGCCGTA -3'. After enzymatic digestion by *Sph*I and *Sal*I-HF, the amplified *Sin3a* coding sequence was subcloned into the pIVT-T7 vector to generate pIVT-*Sin3a*-T7.

Firefly luciferase reporter constructs under the control of the *Sin3a* 3' untranslated region (3' UTR) were generated as previously described (Ma et al., 2013). Briefly, The entire 1-kb *Sin3a* 3' UTR with a ploy(A) site was amplified using the forward primer 5'-GATATCTAGACTGCAGAGCCAGAGCAGGTAGC-3' and reverse primer 5'-GCGCCGAATTCACTTATTTCCTTAAGAATCAAGCT-3'. Amplified *Sin3a* 3' UTR were digested by *Xba*I and *EcoR*I and subcloned downstream of the coding sequence of the pIVT-*Luc* vector.

In Vitro Transcription

The DNA sequence-verified pIVT-*Sin3a*-T7 construct was linearized by *Sfo*I digestion. Capped cRNAs were made using in vitro transcription with T7 mMESSAGE mMachine (Ambion) according to the manufacturer's instructions. Following in vitro transcription, template plasmid DNAs were digested by adding RNase-free DNase and the synthesized cRNA were purified by MEGAclear Kit (Ambion), precipitated and redissolved in RNase-free water.

The DNA sequence verified pIVT-firefly *Luc*/*Sin3a* 3' UTR construct was linearized by *EcoR*I digestion. The linearized product was then processed as described above. For both constructs, a single cRNA band of the expected size

was observed for each cRNA sample following electrophoresis in an 1% formaldehyde denaturing agarose gel. Synthesized cRNA was aliquoted and stored at -80 °C. For microinjection controls, polyadenylated *Renilla luciferase* cRNA was generated by using a *Not*I linearized *Renilla* luciferase based vector phRL-SV40 (Promega). The lineralized vector was in vitro transcribed by T7, and then polyadenylated by Poly(A) Tailing Kit (Ambion) according to the manufacturer's instructions. After polyadenylation and electrophoresis on 1% formaldehyde denaturing agarose gel, it was estimated that approximately a 150 bp poly(A) tail was added to the 3' terminus of the *Renilla* Luc cRNA (Ma et al., 2013).

Luciferase Reporter Assay

Full-grown GV-intact oocytes were microinjected with 5 pl of a solution containing pIVT-firefly *Luc*/*Sin3a* 3' UTR cRNA (0.365 ug/μl) and control *Renilla Luc* cRNA (0.075 ug/μl) (Ma et al., 2013). Injected oocytes were transferred to milrinone-free CZB medium and matured in vitro for 18 h. Injected GV oocytes cultured for 18 h in CZB supplemented with 10 uM milrinone served as controls. In addition to injecting GV full-grown oocytes, MII eggs were microinjected with 5 pl of the same cRNA mixture. Injected MII eggs were activated with 5 mM strontium chloride in modified CZB medium that is free of Ca^{2+} and Mg^{2+} for 6 h at 37 °C under an atmosphere of 5% CO_2 in air. Injected MII eggs cultured in Ca^{2+}- and Mg^{2+}-free CZB medium without $SrCl_2$ for 6 h served as controls. Luciferase activity was assayed by lysing oocytes/eggs/embryos in 1x passive lysis buffer and analyzed using a dual-luciferase reporter assay system (Promega) according to the manufacturer's instructions. For signal normalization, the background firefly/*Renilla* luciferase activity readout from noninjected oocytes/eggs was subtracted, and the firefly luciferase activity was normalized to that of the coinjected *Renilla* luciferase reporter.

Microarrays Analysis

Total RNA was extracted from 20 oocytes/synchronized 2-cell embryos as described above and amplified with the Ovation Pico WTA system V2 (NUGen). The product was then fragmented and labeled with the Encore Biotin Module V2 (NuGen). Four independent biological replicates were hybridized to GeneChip Mouse 2.0 ST microarrays (Affymetrix, Sata Clara, CA, USA).

The microarray datasets from the MoGene-2_0-st (GPL16570) platform were processed using the Oligo package (Carvalho and Irizarry, 2010) from the Bioconductor framework (Gentleman et al., 2004). Raw data was background corrected, normalized and summarized using the robust multi-array average procedure.

Differential expression analysis was done using a robust linear model with empirical Bayes from the limma package (Ritchie et al., 2015). We compared the following conditions: α-amanitin vs. control 2-cell embryo; *Sin3a* KD (knockdown) 2- cell embryo vs. control 2-cell embryo; control 2-cell embryo vs. GV oocyte; and *Sin3a* KD 2-cell embryo vs. GV oocyte. The P-values were calculated using a moderate t-statistic. The calculated P-values were adjusted for multiple testing using the false discovery rate procedure. Genes were marked as differentially expressed if they had a minimal absolute fold-change >1.5 and a calculated P-value <0.05.

Platform annotations were downloaded from the Gene Expression Omnibus repository, and all genes that mapped to differentially expressed Affymetrix probesets (defined as false discovery rate <0.05 and absolute logarithmic fold-change >0.58, in any of the comparisons), were kept for further analysis. The 29,680 Affymetrix probesets, which could be annotated, were used for the differential expression analysis, and functional analysis of differentially expressed gene sets was done using the pantherdb database (Mi et al., 2013).

Statistical Analysis

One-way ANOVA were used to evaluate the differences between groups using GraphPad Prism 6 software (GraphPad Software). A level of P-value < 0.05 was considered to be significant.

CHAPTER 3: INHIBITING THE MATURATION-ASSOCIATED INCREASE IN MATERNAL SIN3A IMPAIRS THE REPORGRAMMING OF GENE EXPRESSION DURING MOUSE PREIMPLANTATION DEVELOPMENT

Research presented in this chapter was carried out in collaboration with the laboratory of Monica Mainigi and Kristian Vlahoviček/Petr Svoboda. Total RNA extraction, amplification, fragmentation and labeling for microarray analysis were performed by Jun Ma, a postdoctoral fellow in the Schultz laboratory. Microarray analysis was performed by Vedran Franke, a doctoral student in the Kristian Vlahoviček laboratory. Olga Davydenko, a postdoctoral fellow in the Mainigi laboratory, performed the embryo transfer experiments.

This work was originally published in Biology of Reproduction. Richard Jimenez, Eduardo O. Melo, Olga Davydenko, Jun Ma, Monica Maingi, Vedran Franke, and Richard M. Schultz. Maternal SIN3A regulates reprogramming of gene expression during mouse preimplantation development. Biology of Reproduction. 2015. 93(4): 89, 1-12.

3.1 Results

3.1a *Sin3a* is a dormant maternal mRNA that is recruited for translation during oocyte maturation and following fertilization

To gain a sense of when the *Sin3a* gene could be functioning, we analyzed the temporal pattern of *Sin3a* abundance by qRT-PCR using random hexamers in mouse oocytes and embryos. The observed differences in relative abundance between the different stages of development will unlikely be attributed to changes in the length of the poly (A) tail of *Sin3a* because random hexamers were used for cDNA synthesis. As with many maternal mRNAs that are degraded during oocyte maturation (Su et al., 2007), *Sin3a* was highly expressed in the full-grown GV intact-oocyte and was degraded upon oocyte maturation as evidenced by the decrease in relative abundance. *Sin3a* abundance reached its lowest level by the 8-cell stage, and between the 8-cell and blastocyst stage,its abundance increased, presumably due to zygotic transcription (Fig. 3.1A). Interestingly, immunoblot analysis of the SIN3A protein revealed a small amount of SIN3A protein present in the full-grown GV-intact oocyte, even though there was an abundant amount of *Sin3a* transcript present at this stage. The amount of SIN3A protein dramatically increased between MI and MII and a further increase was observed following fertilization before a dramatic and rapid loss of SIN3A protein by the 2-cell stage (Fig. 3.1B). The lowest relative abundance of SIN3A protein was observed at the 8-cell stage and then increased by the blastocyst stage, which is consistent with *Sin3a* mRNA relative abundance. It is also noteworthy that this increase in the amount of *Sin3a* transcript and protein by the blastocyst stage nearly coincides with the stage at which *Sin3a* embryonic null embryos (born from *Sin3a*^{+/-} intercrosses) perish.

To better characterize the time course of maternal SIN3A protein loss during early embryonic development, 1-cell and 2-cell mouse embryos were collected for immunoblot analysis. The results showed that the dramatic

reduction in the amount of SIN3A protein occurred as early as the late 1-cell stage (~63% SIN3A loss compared to the mid 1-cell), and continued to the early 2-cell stage (~ 87% SIN3A loss compared to the late 1-cell) and late 2-cell stage, where SIN3A was faintly detected by immunoblot analysis (Fig. 3.2).   Exposure of the embryos to MG132, a proteasome inhibitor, significantly inhibited the reduction in the amount of SIN3A protein, suggesting that the loss of maternal SIN3A protein is potentially mediated by the proteasome (Fig. 3.3).

Immunocytochemical detection of SIN3A protein revealed that the SIN3A protein was nuclear, present in both pronuclei at the 1-cell stage, present in the nuclei of both the TE and ICM cells at the blastocyst stage, and had a similar pattern of expression as revealed by immunoblot analysis (Fig. 3.4). The localization of the SIN3A protein remained nuclear in the male and female pronuclei even after the 1-cell mouse embryos were permeabilized prior to fixation (Fig. 3.5), indicating that the SIN3A protein is likely associated with the chromatin in both pronuclei.

The results described above indicate that *Sin3a* is a dormant maternal mRNA that is recruited for translation during oocyte maturation and following fertilization. In mouse, recruitment of transcripts for translation during oocyte maturation is driven by sequences within the 3' untranslated region (3' UTR) of their respective transcripts, e.g., cytoplasmic polyadenlyation elements (CPEs) (Oh et al., 2000). Given the increase in the relative abundance of SIN3A protein between the full-grown GV-intact oocyte and the MII egg and the presence of CPEs within the 3' UTR of the *Sin3a* transcript, we measured the luciferase activity of lysed MII eggs following maturation of full-grown GV-intact oocyte microinjected with firefly luciferase reporter cRNA under the control of the *Sin3a* 3' UTR. This experiment revealed a dramatic increase in luciferase activity following maturation of oocytes microinjected with the luciferase reporter cRNA (Fig. 3.6A). An increase in luciferase activity following microinjection of the cRNA and later activation of MII eggs was also observed (Fig. 3.6B), which is consistent with the observed increase in the relative abundance of the SIN3A

protein following fertilization.

3.1b Inhibiting the maturation-associated increase in SIN3A alters global H3 and H4 histone acetylation in 1-cell embryos

Because SIN3A is a part of the SIN3A-co-repressor complex and the results described above suggesting that the function of SIN3A is restricted mainly to the 1-cell stage, we wanted to assess whether the loss of maternally recruited SIN3A had an effect on histone acetylation at the 1-cell stage. We utilized a combined morpholino/siRNA approach to inhibit the oocyte maturation-associated increase in SIN3A. Following oocyte maturation of full-grown GV-intact oocytes microinjected with the morpholino/siRNA sample targeted against the *Sin3a* transcript, no increase in the amount of SIN3A protein was seen (Fig. 3.7). As a control, when a scramble siRNA and a standard morpholino were injected into the full-grown oocyte, a normal maturation-associated increase in SIN3A was observed (Fig. 3.7). These results show that this approach can effectively inhibit the maturation-associated increase in SIN3A.

Because the epigenetic modifications of the male and female genomes are distinct at fertilization and during the first cell cycle of early embryo development as described above (Santos et al., 2005; Erhardt et al., 2003; Lepikhov and Walter, 2004; Liu et al., 2004) and the results above suggest that SIN3A is chromatin-associated in both male and female pronuclei (Fig. 3.5), it is plausible that SIN3A may have differential effects on the chromatin of each pronuclei. To determine if the inhibition of the maturation-associated increase in SIN3A affected global histone acetylation in 1-cell embryos and to determine if the effects were dependent on the parental origin of the chromatin, we performed immunocytochemistry analysis of 1-cell embryos generated by in vitro insemination of in vitro matured, microinjected oocytes rather than activation of the oocytes. Also, because in vitro insemination results in asynchronous 1-cell embryo formation due to differences in the timing of fertilization and because the appearance of histone post-translation modifications during the 1-cell stage is

dependent on the stage of pronuclear development, highly synchronized 1-cell embryos were used for immunocytochemistry analysis to minimize cell-cycle differences.

We assessed global H3K18ac, H4K5ac, H4K8ac, H4K12ac and H4K16ac in highly synchronized 1-cell embryos because many of these marks are affected in mouse embryos when HDAC function is perturbed (Ma and Schultz, 2008) and because these histone modifications represent three distinct regions of genes; H3K18ac is enriched in the region surrounding the transcriptional start site, whereas the others are enriched in the promoter and transcribed regions of active genes (Wang et al., 2008). Interestingly, the enrichment of H4K12ac in transcribed regions is associated with transcriptional elongation (Cho et al., 1998). Although a moderate hyperactylation of all these marks globally was observed when 1-cell embryos were incubated in the presence of Trichostatin A, an HDAC inhibitor, such was not the case when the maturation-associated increase in SIN3A was inhibited (Fig. 3.8). Surprisingly, we observed a modest hypoacetylation for global H3K18ac, H4K8ac and H4K12ac.

3.1c Inhibiting the maturation-associated increase in SIN3A impairs development beyond the 2-cell stage

Next, we assessed the effect of inhibiting the maturation-associated increase in SIN3A on preimplantation development. After blocking the maturation associated-increase in SIN3A, the embryos depleted of maternally recruited SIN3A developed poorly beyond the 2-cell stage when compared to the control-injected embryos (Fig. 3.9). The deleterious effects on development of subjecting denuded, microinjected oocytes to in vitro maturation and insemination is the likely explanation for the low incidence of development in the control group. The arrest at the 1-cell and 2-cell stages in the experimental group is unlikely due to a failure to undergo DNA replication because essentially all of the experimental and control embryos at both the 1-cell and 2-cell stages incorporated BrdU, and based on comparable signal intensities of BrdU

incorporation, each group replicated their DNA to a similar extent (Fig. 3.10).

In mice, impairment of ZGA and a reduction in transcription by at least 70% by α-amanitin leads to developmental arrest at the 2-cell stage (Flach et al., 1982; Bolton et al., 1984; Schultz, 1993; Ma et al., 2001). To determine whether the developmental arrest observed was due to inhibiting transcription at a global level, we assessed global transcription by EU incorporation after inhibiting the maturation-associated increase in SIN3A in highly synchronized 2-cell embryos. We observed that transcription was reduced by 50% in the experimental 2-cell embryos when compared to the control 2-cell embryos (Fig. 3.11). It is unlikely that the developmental arrest at the 2-cell stage was due to inhibiting global transcription because a 50% reduction in transcription is not sufficient to lead to a developmental arrest at the 2-cell stage.

Because transcription in 1-cell embryos is required for development beyond the 2-cell stage but is dispensable for cleavage to the 2-cell stage (Abe et al., 2015), we assessed global transcription by EU incorporation in 1-cell embryos. No effect on transcription in either the maternal or paternal pronucleus of 1-cell embryos was observed after blocking the maturation-associated increase in SIN3A (Fig. 3.12).

3.1d Impairment of gene expression reprogramming in maternal SIN3A-depleted embryos

In mice, a dramatic reprogramming of gene expression accompanies ZGA during the 2-cell stage and failure to successfully reprogramming the genome is associated with a developmental arrest at the 2-cell stage (Bultman et al., 2006). To examine whether the reprogramming of gene expression was affected, we carried out genome-wide expression profiling of control full-grown GV-intact oocytes, highly synchronized control and maternal SIN3A-depleted 2-cell embryos cultured with or without the transcriptional inhibitor α-amanitin. Because SIN3A regulates expression of its target genes, we expected that a subset of zygotically activated genes would be affected in 2-cell embryos. The

zygotically activated genes are genes whose expression is inhibited by α-amanitin.

As expected, hierarchical cluster analysis did not reveal significant differences between the transcriptomes of the full-grown GV intact-oocytes and 2-cell embryos treated with α-amanitin (Fig. 3.13). However, the transcriptomes of both these groups differed significantly from the transcriptomes of the control and experimental 2-cell embryos. Importantly, the transcriptomes of the control and maternal SIN3A-depleted 2-cell embryos differed significantly from each other, which is consistent with the prediction that a subset of zygotically activated genes would be impaired when maternal SIN3A is depleted from the embryo.

Because formation of a histone hyperacetylation responsive transcriptionally repressive state may decrease expression of inappropriately activated genes and because SIN3A may have a role in formation of the repressive state, we identified zygotically activated genes whose expression was higher in maternal SIN3A-depleted embryos. We found 145 zygotically expressed genes whose expression was at least 1.5-fold higher in 2-cell embryos derived from eggs in which the maturation-associated increase in SIN3A was inhibited (Table 3.1). Not only were protein-coding genes included in the list of 145 genes, but ribosomal genes, small nuclear RNAs, and noncoding RNAs were also present.

Because formation of a transcriptionally repressive state may also terminate expression of inappropriately activated genes in mouse 2-cell embryos, it is likely that genes, which were not normally zygotically activated in 2-cell embryos, were now inappropriately expressed in 2-cell embryos depleted of maternal SIN3A. These genes would show no difference in expression between control and α-amanitin-treated 2-cell embryos, but would show an increased expression in maternal SIN3A-depleted embryos when compared to control embryos. We found 98 genes that were not zygotically activated in 2-cell embryos, but whose expression was increased in maternal SIN3A-depleted 2-cell embryos (Table 3.2). These genes included protein coding genes, ribosomal

genes, small nuclear RNAs, noncoding RNAs, small nucleolar RNAs, and microRNAs. The qRT-PCR on four transcripts from each class whose expression was increased by inhibiting the maturation-associated increase in SIN3A revealed changes in relative transcript abundance similar to that observed from the microarray data for all of them except for one (Table 3.3). These results afford confidence that differences observed in the microarray data analysis reflect changes in relative transcript abundance.

To determine if the dysregulated genes identified in the 2-cell embryos depleted of maternal SIN3A form gene clusters, the genes whose expression was increased in maternal SIN3A-depleted embryos were mapped to chromosomes. As expected, the misexpressed genes mapped within chromosomal gene clusters, with enrichment of these genes on some chromosomes (e.g., chromosome 11 and 12) (Fig. 3.14).

3.1e Exogenously expressing SIN3A beyond the 1-cell stage does not impair preimplantation development

The restricted presence of maternal SIN3A protein mainly to the 1-cell stage is unique because other maternal proteins that are encoded by dormant maternal mRNAs are present for much longer periods of time. It is likely that restricting the function of maternal SIN3A mainly to the 1-cell stage and the precipitous reduction in the amount of SIN3A protein are required for development beyond the 2-cell stage. Accordingly, we assessed the effect of maintaining the presence of SIN3A beyond the 1-cell stage. After microinjecting cRNA encoding *Sin3a* into 1-cell mouse embryos at different concentrations, we identified the conditions that allowed for an increase in the amount of SIN3A protein in 2-cell embryos to an amount that is comparable to that observed following oocyte maturation and fertilization (Fig. 3.15A).

Because SIN3A protein is not stable during mouse preimplantation development, we decided to use 1-cell embryos microinjected with a buffer as the control group because a typical control would involve microinjecting a cRNA

encoding some protein that is usually stable, which SIN3A is not. Furthermore, we observed that the developmental incidence to the blastocyst stage depended on what control cRNA was microinjected (Fig. 3.15C). Results from these experiments showed that development to the blastocyst stage was not affected by maintaining the presence of SIN3A protein beyond the time when it has normally decreased to undetectable levels (Fig. 3.15B). In addition, total cell numbers and their types (epiblast, ICM, trophectoderm) in blastocysts were not affected (Fig. 3.16).   Furthermore, the blastocysts from microinjected 1-cell embryos that maintained elevated levels of SIN3A protein beyond the 1-cell stage had a similar incidence of implantation and resorption as the control groups when embryo transfer experiments were performed (Fig. 3.17).
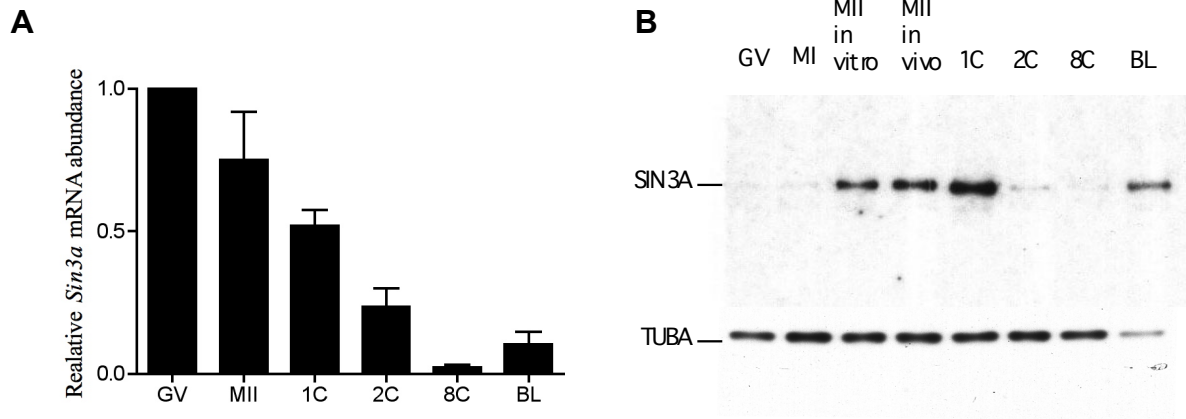
Figure 3.1. Developmental expression profile of Sin3a/SIN3A.

(**A**) *Sin3a* mRNA levels were measured by quantitative RT-PCR at the indicated stages. Data were normalized against the detected levels of exogenously added *GFP* and expressed relative to the value obtained for mid 1-cell embryos. The experiment was conducted three times and the data are expressed as mean ± SEM. GV, full-grown GV-intact oocytes; MII, metaphase II-arrested egg; 1C, 2C, and 8C refer to 1-cell, 2-cell, and 8-cell stages, respectively; BL, blastocyst. (**B**) The relative amount of SIN3A was measured by immunoblot analysis. MII *in vitro*, oocytes were matured *in vitro* to MII; MII *in vivo*, MII eggs were collected following maturation *in vivo*. The TUBA signal was used to normalize total protein loading. The experiment was performed three times and similar results were obtained in each case. A representative example is shown.

A

B
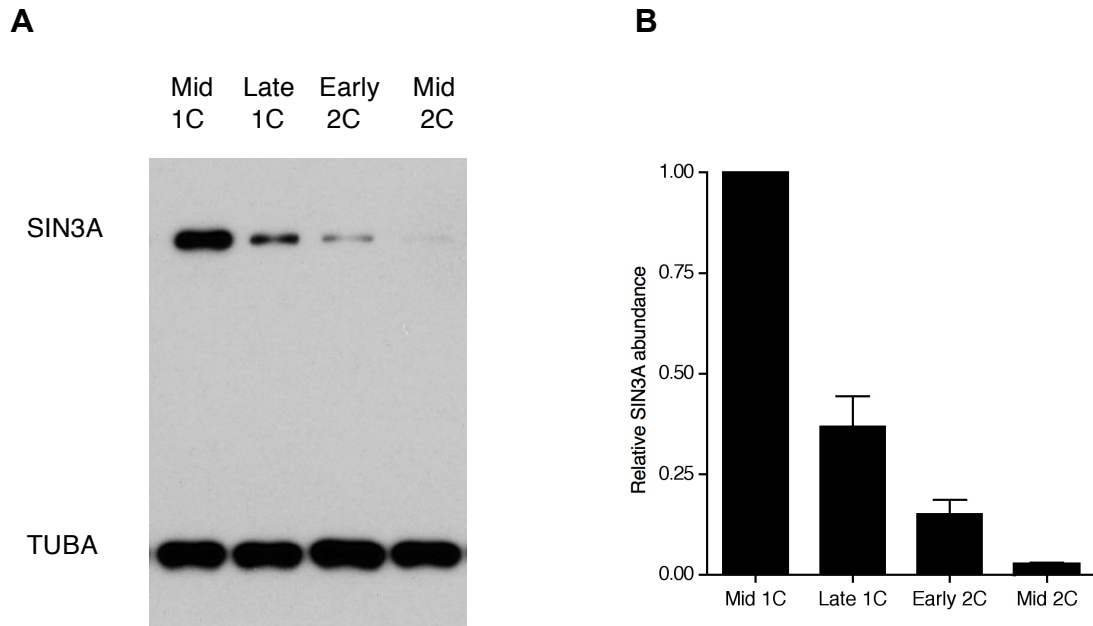
Figure 3.2. **Time course for SIN3A protein loss.**

(A) Immunoblot analysis for SIN3A was conducted at the indicated developmental stages. The TUBA signal was used to normalize total protein loading. The experiment was performed three times and similar results were obtained in each case; shown is a representative example. (**B**) Quantification of the data shown in A. The data are expressed as the mean ± SEM and the SIN3A signal is relative to the mid 1-cell embryo.
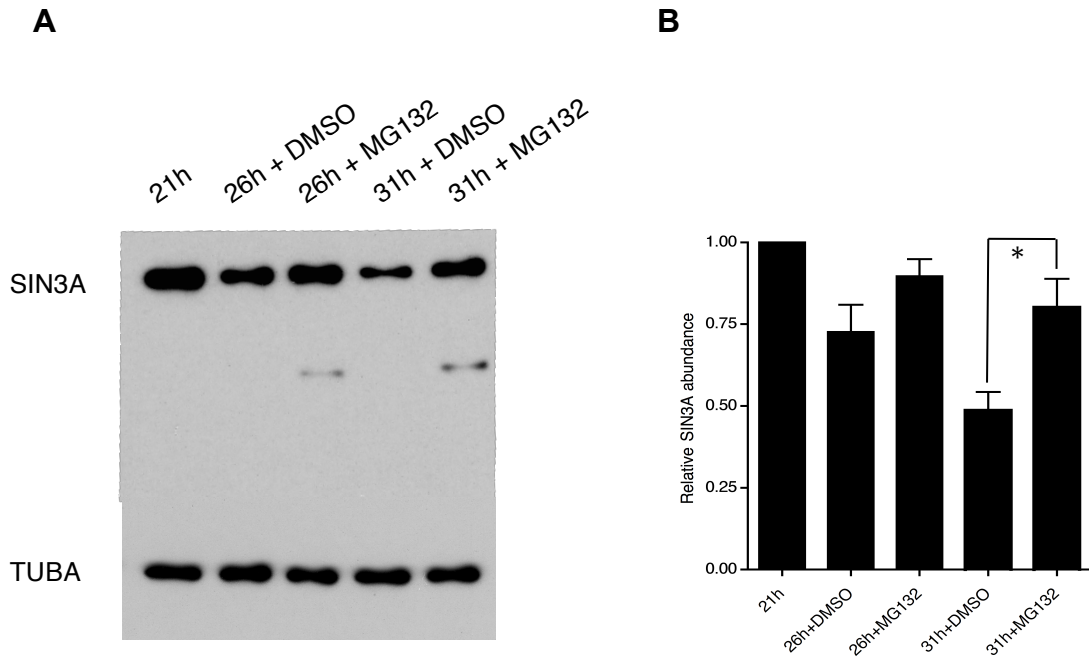
Figure 3.3. SIN3A protein loss is proteasome-dependent

(**A**) Mid 1-cell embryos were isolated and cultured *in vitro* in the presence of the proteasome inhibitor MG132 or DMSO, the vehicle. SIN3A protein abundance was measured by immunoblot analysis at the indicated times. The TUBA protein signal was used to normalize total protein loading. The experiment was performed three times and a representative example is shown. (**B**) Quantification of the data shown in A. The data are expressed as the mean ± SEM and the SIN3A signal is relative to the mid 1-cell embryo. The times refer to the number of hours post-hCG injection. * $P < 0.05$.
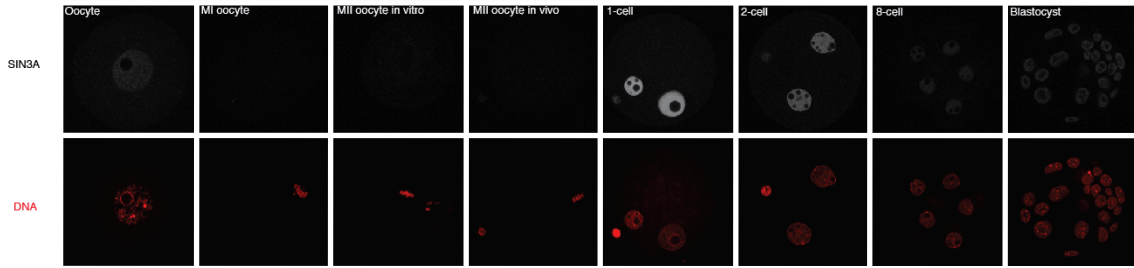
Figure 3.4. Developmental expression profile of SIN3A protein by immunocytochemistry.

Immunocytochemical analysis of SIN3A expression during preimplantation development. The experiment was conducted two times, and at least 15 oocytes/embryos were analyzed for each experiment.
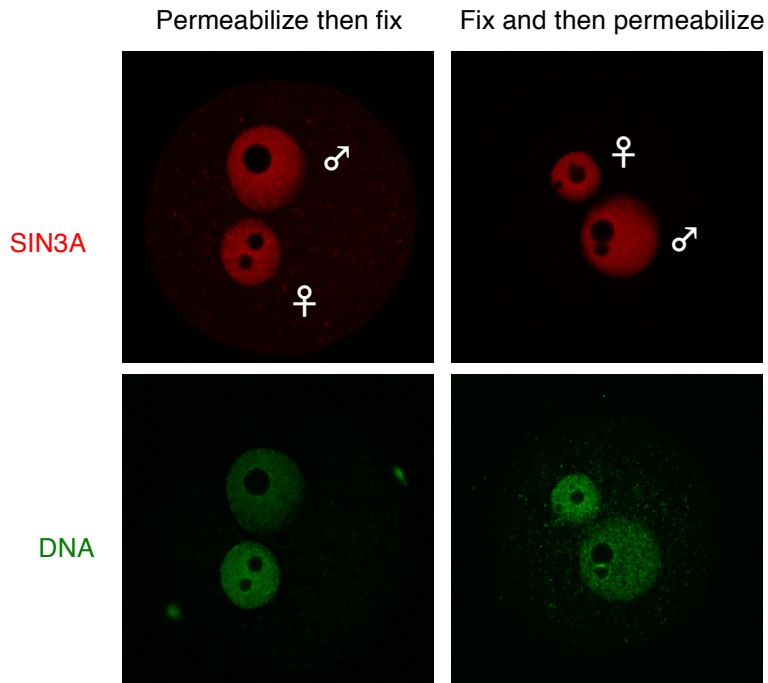
Figure 3.5. Similiar amount of chromatin-associated SIN3A protein between male and female pronuclei.

Immunocytochemical detection of chromatin-associated SIN3A was performed by permeabilizing and then fixing 1-cell embryos and the signal was then compared to the signal obtained when the 1-cell embryos were fixed and then permeablized. Shown are representative images in which there is no obvious difference for the two different protocols.

A

B
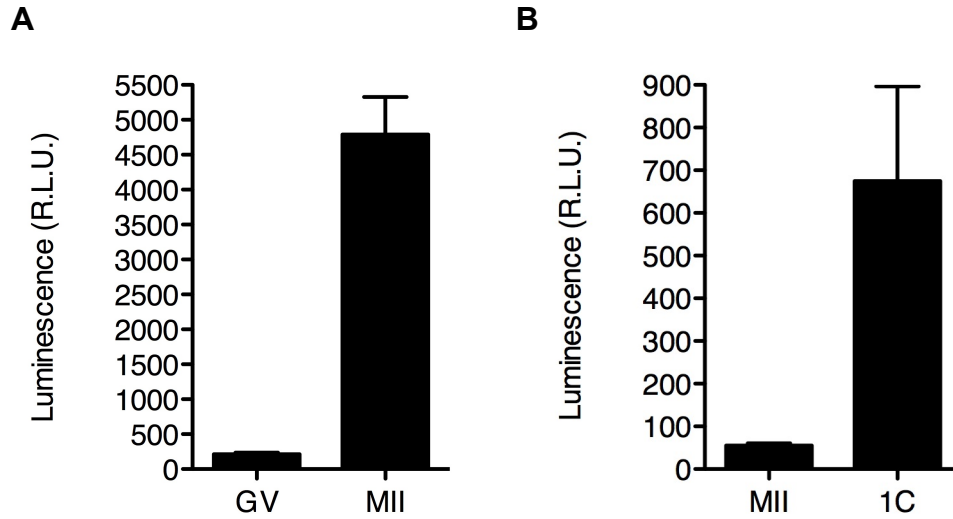
Figure 3.6. *Sin3a* **3'UTR contains elements that drive translational recruitment during oocyte maturation and following activation.**
Full-grown oocytes (**A**) or MII eggs (**B**) were microinjected with the luciferase reporter cRNAs. Firefly luciferase reporter activities were normalized to the co-injected Renilla luciferase. The data are expressed as mean ± SEM, and at least 10 oocytes/embryos were analyzed for each group.
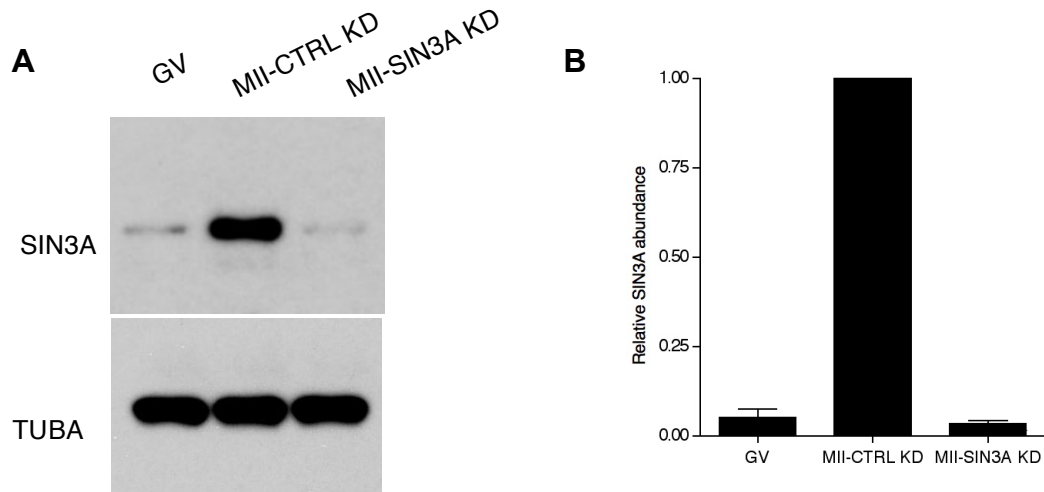
Figure 3.7. Combined *Sin3a* morpholino and siRNA inhibit maturation-associated increase in the amount of SIN3A protein.

(**A**) Full-grown oocytes microinjected with control or *Sin3a* morpholino (MO) and siRNA were cultured for 1 h in medium containing 2.5 μM milrinone and then cultured in inhibitor-free medium for maturation. MII eggs were collected 16 h after maturation and used for immunoblot analysis to detect SIN3A protein levels. TUBA was used to normalize total protein loading. The experiment was performed three times and a representative example is shown. (**B**) Quantification of the relative amount of SIN3A shown in panel A. The data are expressed as mean ± SEM.
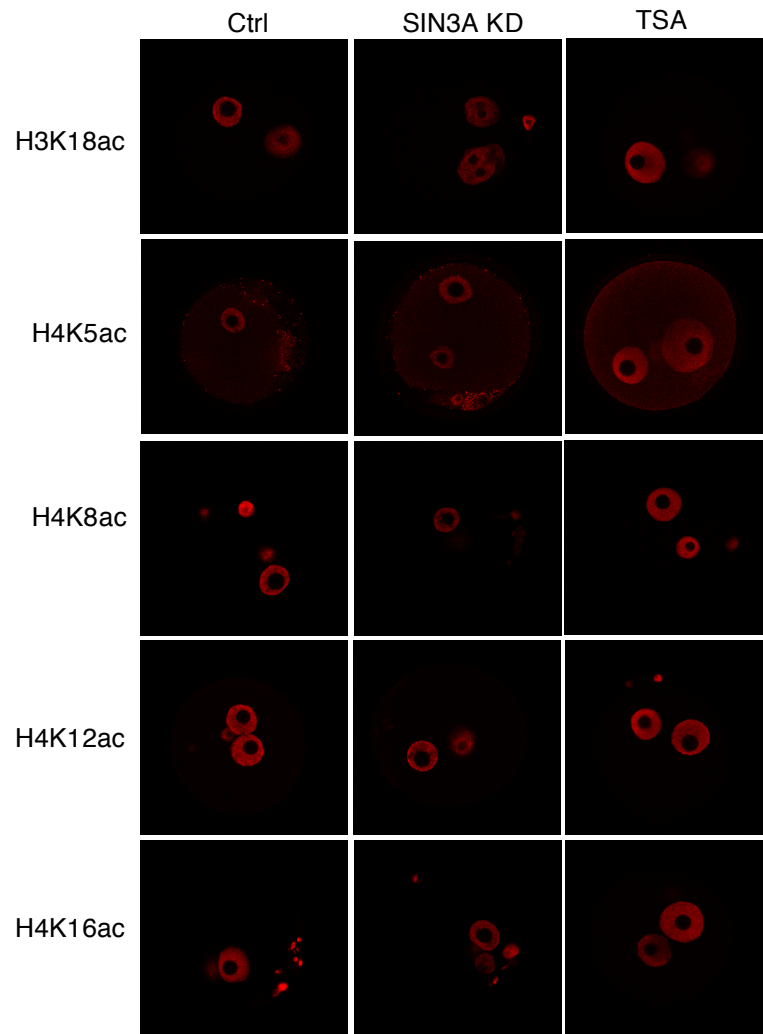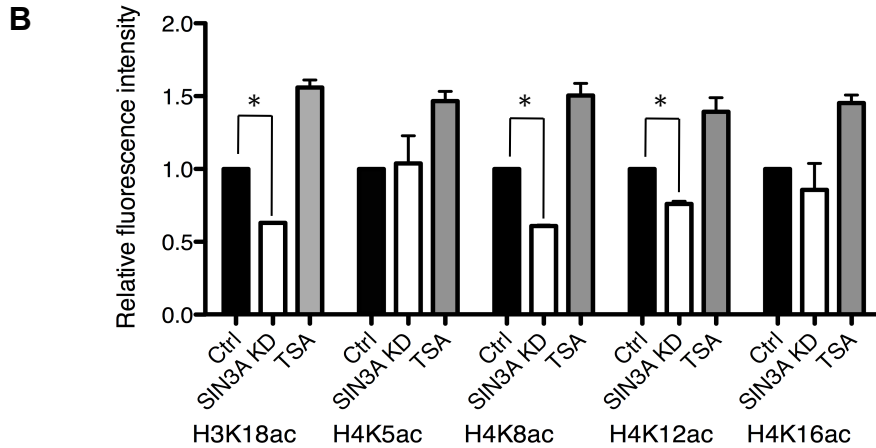
Figure 3.8. Effect of inhibiting the maturation-associated increase in SIN3A on histone acetylation in 1-cell embryos.

(**A**) The indicated histone were assayed by immunocytochemistry for their acetylation status using maternal-SIN3A depleted 1-cell embryos, control 1-cell embryos, and 1-cell embryos that were incubated with Trichostatin A (an HDAC inhibitor) to generate the maximum increase in histone acetylation. The experiment was performed two times and at least a total of 10 embryos were analyzed for each sample group. (**B**) Quantification of the data shown in panel A. The data are expressed relative to the control 1-cell embryos and are expressed as mean ± SEM. *, $p < 0.05$.
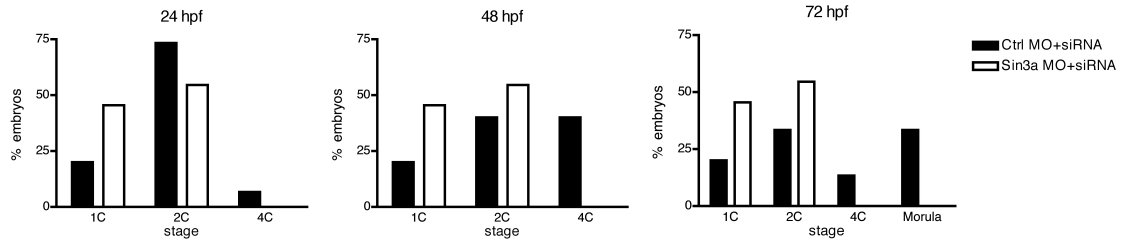
Figure 3.9. Inhibiting the maturation-associated increase in SIN3A protein leads to a developmental arrest at the 2-cell stage.

After inhibiting the maturation-associated increase in SIN3A protein, the maternal-SIN3A depleted and control MII eggs were *in vitro* fertilized (IVF) and embryo development was assessed at 24, 48 and 72 h after fertilization. The experiment was performed three times and the data pooled. A total of 56 experimental and 43 control embryos were analyzed. hpf, hours post-fertilization.
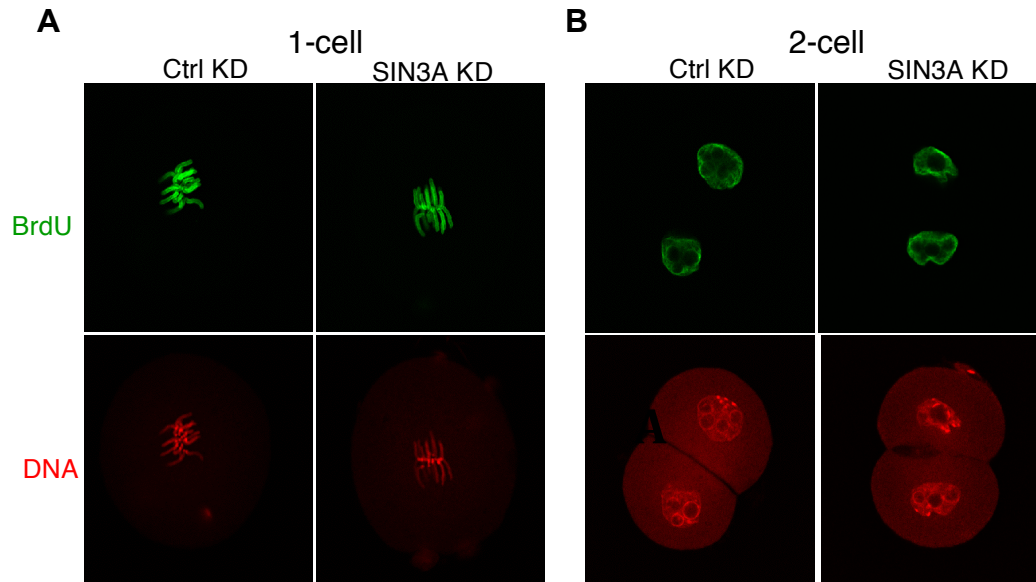
Figure 3.10. DNA replication is not inhibited in 1- and 2-cell embryos when the maturation-associated increase in SIN3A protein is inhibited.
After inhibiting the maturation-associated increase in SIN3A protein, the maternal-SIN3A depleted and control MII eggs were *in vitro* fertilized (IVF) and placed in medium containing BrdU, a deoxyribonucleotide analog incorporated into DNA. Controls were injected with control siRNA and morpholino. BrdU incorporation was assayed by immunocytochemistry in 1-cell and 2-cell embryos. The experiment was conducted two times, and at least 10 embryos were analyzed for each experiment.
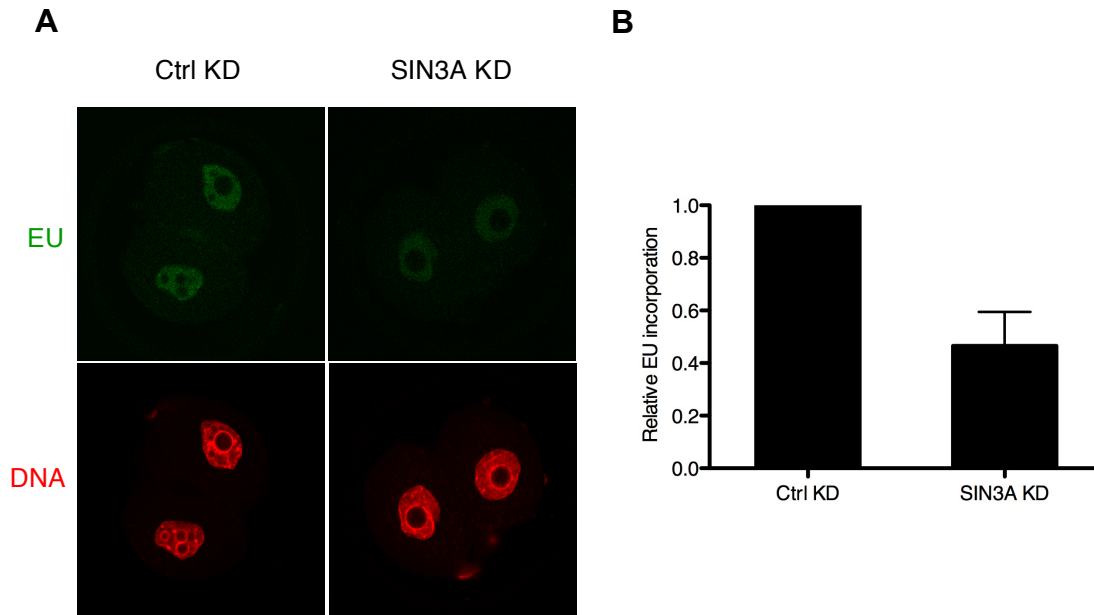
Figure 3.11. Transcription is reduced in 2-cell embryos depleted of maternal-SIN3A.

(**A**) After inhibiting the maturation-associated increase in SIN3A protein, the maternal-SIN3A depleted and control MII eggs were *in vitro* fertilized (IVF) and placed in medium containing EU, a ribonucleotide is incorporated into nacent RNA. Controls were injected with control siRNA and morpholino. EU incorporation was assayed by immunocytochemistry in 2-cell embryos. The experiment was performed 4 times and shown are representative images. At least 10 embryos were analyzed for each treatment group. (**B**) Quantification of the images shown in panel A. The data are expressed as mean ± SEM. * $p < 0.05$.
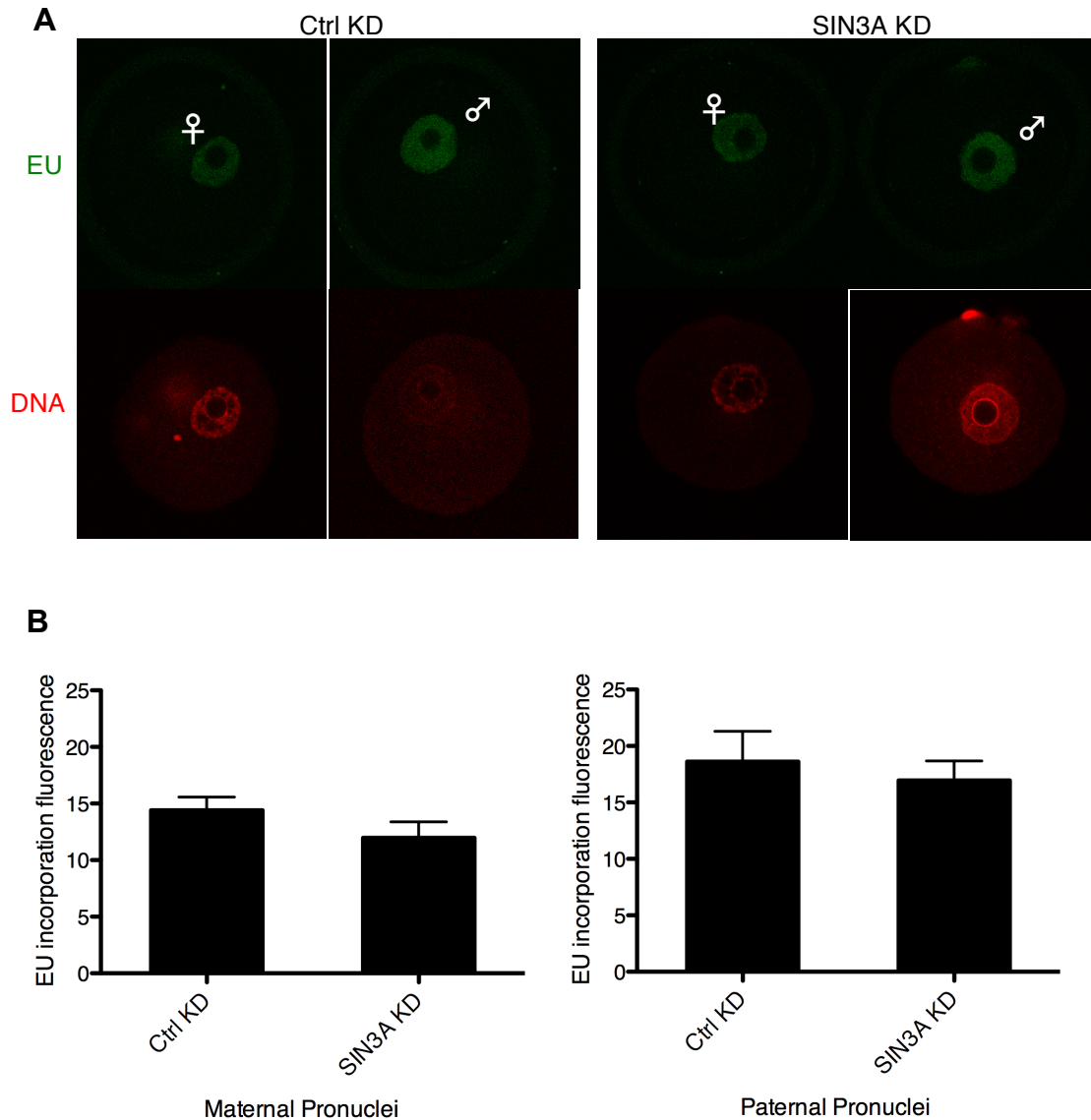
Figure 3.12. No change in global transcription at the 1-cell stage when the maturation-associated increase in maternal SIN3A is inhibited.

(**A**) Immunocytochemical detection of EU incoportation in maternal-SIN3A depleted and control 1-cell embryos. Shown are representative images. The experiment was conducted two times, and at least 10 embryos were analyzed for each experiment. (**B**) Quantification of the data shown in panel A. The data are expressed as mean ± SEM.
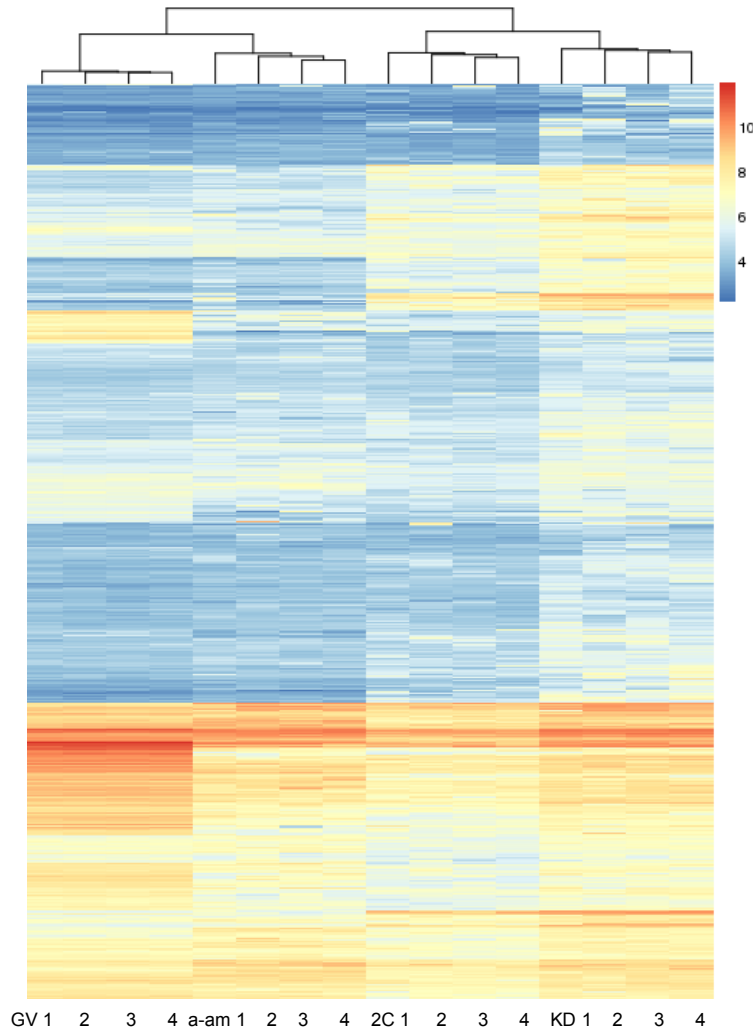
Figure 3.13. Heat map of all samples from different treatment groups constructed using hierarchical clustering.

Replicate sample numbers are indicated at the bottom of the figure. GV, full-grown GV-intact oocytes; a-am, 1-cell embryos incubated in α-amanitin to the 2-cell stage; 2C, 2-cell embryos derived from oocytes injected with control siRNA and morpholino matured and fertilized in vitro; KD, 2-cell embryos derived from oocytes injected with *Sin3a* siRNA and morpholino matured and fertilized in vitro. Colors correspond to relative RNA abundance (on the log2 scale) for the detected genes each of which is represented by one horizontal bar. The numbers correspond to each replicate within each group.
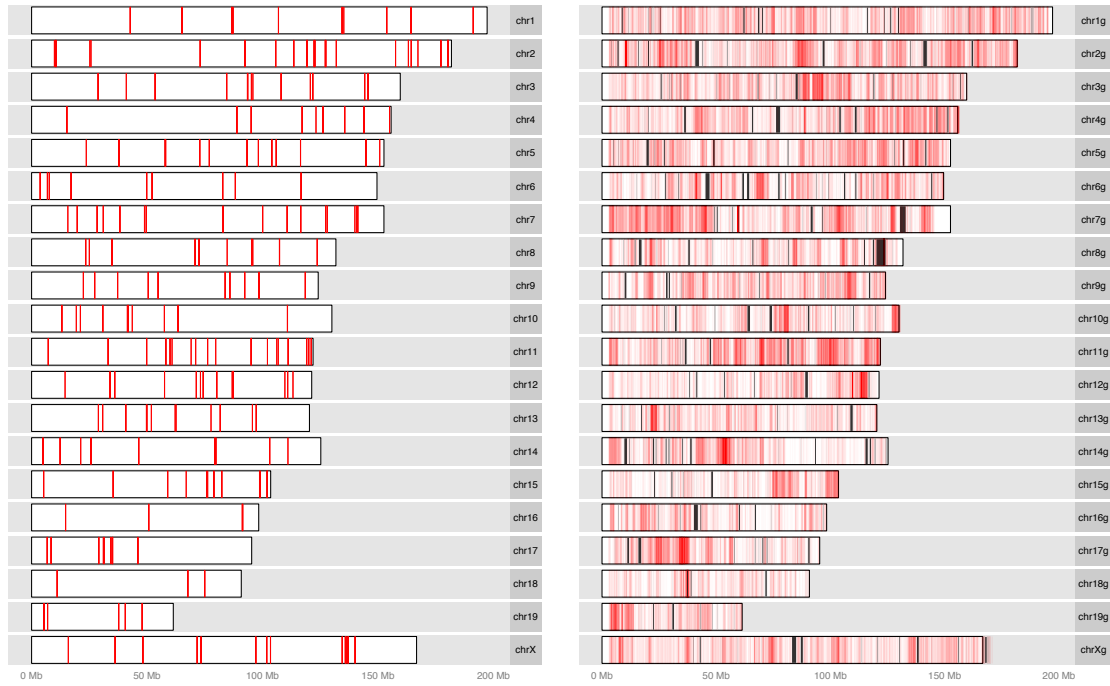
Figure 3.14 Karyogram of genes whose expression was elevated in 2-cell embryos depleted of maternal SIN3A (left panel) and density of genes (right panel).

The comparison showed that most of the SIN3A sensitive genes emanated from gene dense regions.
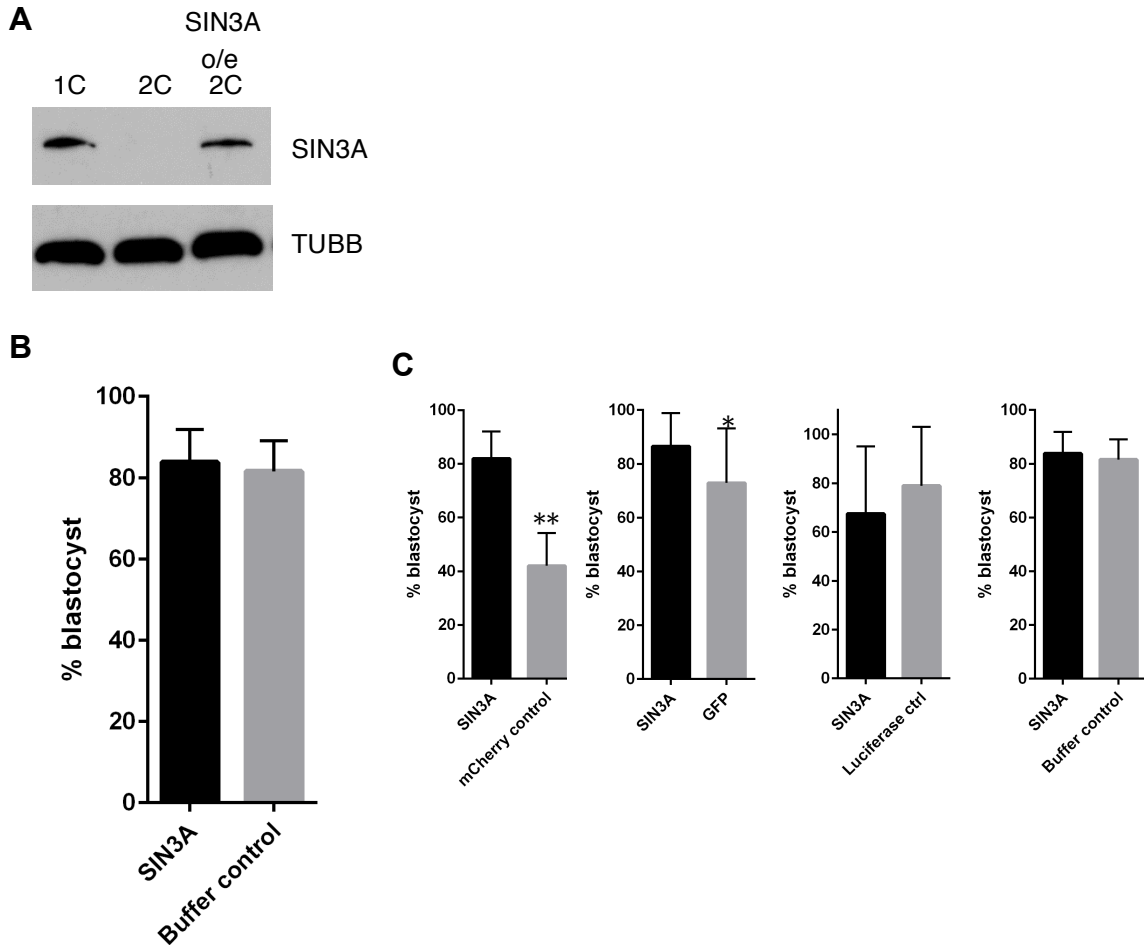
Figure 3.15. Over-expressing SIN3A does not affect pre-implantation development.

(**A**) One-cell embryos were microinjected with cRNA encoding *Sin3a* and were cultured to the 2-cell stage and used for immunoblot analysis to detect SIN3A protein levels. Control embryos were injected with buffer. TUBB was used to normalize total protein loading. The experiment was performed three times and a representative example is shown. (**B**) Effect of over-expressing SIN3A on development to the blastocyst stage. Control embryos were injected with buffer. The experiment was conducted 7 times and at least 261 embryos were analyzed in each group. The data are expressed as mean ± SEM. (**C**) One-cell embryos were microinjected with either a cRNA encoding *Sin3a*, a cRNA encoding

mCherry, Gfp, or Luc, or buffer. The incidence of development to the blastocyst was then assessed. The experiment was performed 4 times using the mCherry control with at least 85 embryos examined for each treatment group, 15 times using the GFP control with at least 292 embryos examined for each treatment group, 2 times using the Luciferase control (ctrl) with at least 76 embryos examined for each treatment group, and 7 times using the buffer control with at least 261 embryos examined for each treatment group. The data are expressed as mean ± SEM. *P <0.05; **P < 0.01.
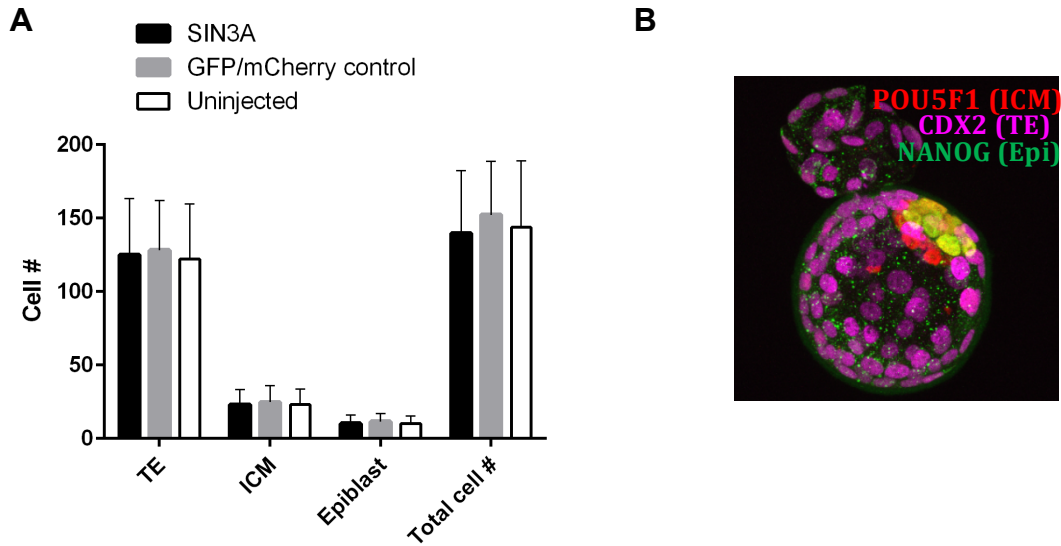
Figure 3.16. Over-expressing SIN3A does not affect cell numbers in blastocysts.

(**A**) Effect of over-expressing SIN3A on cell numbers in blastocysts. The experiment was conducted 4 times and at least 32 embryos were analyzed in each group. The data are expressed as mean ± SEM. (**B**) Immunocytochemical detection of lineage markers in blastocysts derived from embryos over-expressing SIN3A.
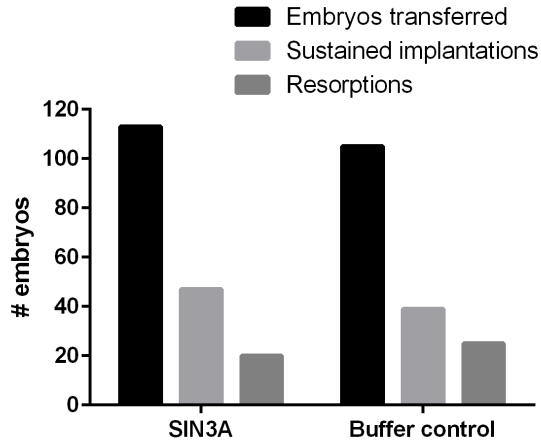
Figure 3.17. Over-expressing SIN3A does not affect pre-implantation development.

One-cell embryos were microinjected with cRNA encoding *Sin3a* or buffer and were cultured to the blastocyst stage. The incidence of post-implantation development following blastocyst transfer of control and SIN3A-over-expressing embryos was then assessed. The experiment was conducted 6 times.

Table 3.1. Zygotically expressed genes whose expression is up-regulated following inhibition of the maturation-associated increase in SIN3A.

Annotation			
ID	SPOT ID	Gene name	Biotype
17446058	chr5(-):23674289-23674381	5S_rRNA	rRNA
17397331	chr3(+):40992693-40992850	U1	snRNA
17481770	chr7(+):110627661-110629819	Adm	protein_coding
17276375	chr12(+):74284276-74295950	1700086L19Rik	protein_coding
17344122	chr17(-):34952013-34952075	1110038B12Rik	processed_transcript
17520624	chr9(+):98422961-98446551	Rbp1	protein_coding
17249036	chr11(+):49794155-49838620	Gfpt2	protein_coding
17517416	chr9(+):54764748-54773110	Crabp1	protein_coding
17327030	chr16(+):91225550-91228677	Olig2	protein_coding
17415345	chr4(+):88799575-88801130	Gm13285	protein_coding
17517097	chr9(+):50494525-50505639	1600029D21Rik	protein_coding
17278767	chr12(+):109643748-109643818	SNORD113	snoRNA
17375880	chr2(+):127363208-127367221	Adra2b	protein_coding
17218889	chr1(+):164249046-164265385	Slc19a2	protein_coding
17355443	chr18(-):74939322-74961263	Lipg	protein_coding
17410974	chr3(-):145646971-145649985	Cyr61	protein_coding
17212313	chr1(+):42697146-42700210	Pou3f3	protein_coding
17510563	chr8(-):72477995-72492614	Slc35e1	protein_coding
17491396	chr7(-):49631499-49636849	Dbx1	protein_coding
17511130	chr8(-):84661331-84662852	Ier2	protein_coding
17375409	chr2(+):122298900-122302885	Duoxa1	protein_coding
17362121	chr19(-):6922426-6925380	1700019N12Rik	protein_coding

17302483	chr14(+):103070216-103077630	Cln5	protein_coding
17279509	chr12(+):113152012-113153879	Crip1	protein_coding
17312829	chr15(+):78926725-78930465	Lgals1	protein_coding
17497847	chr7(-):141278331-141279133	Sct	protein_coding
17418154	chr4(+):123116248-123118000	Oxct2b	protein_coding
17263511	chr11(-):59963181-59964944	Rasd1	protein_coding
17322125	chr15(-):102028228-102029513	Krt18	protein_coding
17237186	chr10(+):110745439-110787384	E2f7	protein_coding
17292011	chr13(-):40715675-40733823	Tcfap2a	protein_coding
17239664	chr10(-):21124930-21160984	Myb	protein_coding
17308939	chr14(-):79766772-79771312	Pcdh8	protein_coding
17386477	chr2(-):72971548-72986716	Gm11084	protein_coding
17395373	chr2(-):177197202-177200415	Gm14391	protein_coding
17397523	chr3(+):53463666-53481755	2810046L04Rik	protein_coding
17406363	chr3(-):84442196-84480439	Fhdc1	protein_coding
17288898	chr13(+):81657806-81671899	Lysmd3	protein_coding
17394175	chr2(-):164424247-164443887	Sdc4	protein_coding
17411961	chr4(+):15265820-15286753	Tmem64	protein_coding
17345293	chr17(-):46016993-46032377	Vegfa	protein_coding
17218321	chr1(+):153740349-153745468	Rgs16	protein_coding
17289372	chr13(+):97241105-97253040	Enc1	protein_coding
17368171	chr2(+):25706879-25707721	A230005M16Rik	processed_transcript
17270053	chr11(-):102106676-102107832	Pyy	protein_coding
17310982	chr15(+):35296098-35303305	Osr2	protein_coding
17470060	chr6(-):116633008-116673836	Rassf4	protein_coding
17394153	chr2(-):164354070-164389095	Slpi	protein_coding

17261542	chr11(-):33117430-33147400	Fgf18	protein_coding
17468018	chr6(-):82725025-82774454	Hk2	protein_coding
17393764	chr2(-):157562361-157562447	Nnat	protein_coding
17291525	chr13(-):28948919-28953713	Sox4	protein_coding
17317313	chr15(-):58890153-58933730	Tatdn1	protein_coding
17544469	chrX(-):134460116-134476490	Taf7l	protein_coding
17399986	chr3(+):93442330-93449077	Tchh	protein_coding
17265470	chr11(-):71031941-71033617	6330403K07Rik	processed_transcript
17240077	chr10(-):30832359-30842801	Hey2	protein_coding
17544816	chrX(-):137115397-137122083	Esx1	protein_coding
17315245	chr15(+):102028216-102032026	Krt18	protein_coding
17455936	chr6(+):6863334-6868568	Dlx6	protein_coding
17500068	chr8(+):23411502-23449632	Sfrp1	protein_coding
17515617	chr9(+):27299228-27334763	Igsf9b	protein_coding
17348400	chr18(+):11052510-11085635	Gata6	protein_coding
17415319	chr4(+):88782131-88783592	Ifnz	protein_coding
17312032	chr15(+):66929607-66931107	Ndrg1	protein_coding
17535535	chrX(+):73342620-73359080	Zfp275	protein_coding
17305709	chr14(-):46383520-46390669	Bmp4	protein_coding
17480620	chr7(+):100006404-100034728	Chrdl2	protein_coding
17303496	chr14(-):12341892-12345865	Fezf2	protein_coding
17260474	chr11(-):7206086-7213923	Igfbp3	protein_coding
17438419	chr5(+):76928368-76947758	2310040G07Rik	processed_transcript
17534051	chrX(+):36112110-36171262	Il13ra1	protein_coding
17510136	chr8(-):70762773-70767151	Ifi30	protein_coding
17367856	chr2(+):25208623-25208727	U6	snRNA
17437049	chr5(+):37820564-37822751	Msx1	protein_coding

17439942	chr5(+):105876565-105915885	Zfp326	protein_coding
17460634	chr6(+):88193891-88207032	Gata2	protein_coding
17227259	chr1(-):135150666-135150766	5S_rRNA	rRNA
17259235	chr11(+):119942763-120006782	Baiap2	protein_coding
17484601	chr7(+):140835018-140837968	1190003J15Rik	protein_coding
17488458	chr7(-):28376784-28379255	Zfp36	protein_coding
17287361	chr13(+):51846675-51848475	Gadd45g	protein_coding
17360216	chr19(+):47854970-47864790	Gsto1	protein_coding
17529307	chr9(-):83778692-83806305	Elovl4	protein_coding
17323192	chr16(+):14705852-14709395	Snai2	protein_coding
17295130	chr13(-):95601789-95618459	F2r	protein_coding
17489399	chr7(-):31032722-31042481	Fxyd5	protein_coding
17335467	chr17(+):29090979-29100722	Cdkn1a	protein_coding
17273447	chr11(-):121053423-121063569	Sectm1b	protein_coding
17410809	chr3(-):144188530-144205255	Lmo4	protein_coding
17482095	chr7(+):116504374-116540588	Nucb2	protein_coding
17479834	chr7(+):82867333-82871576	Mex3b	protein_coding
17483258	chr7(+):127244526-127254803	Zfp771	protein_coding
17255352	chr11(+):95120089-95125296	Dlx3	protein_coding
17417622	chr4(+):117096075-117115383	Ptch2	protein_coding
17286231	chr13(+):28943048-28951671	Sox4	protein_coding
17402144	chr3(+):120683970-120693602	Usp12	protein_coding
17388353	chr2(-):92365046-92371057	Gyltl1b	protein_coding
17544919	chrX(-):140006805-140062712	Nup62cl	protein_coding
17344114	chr17(-):34950235-34952471	1110038B12Rik	processed_transcript
17505260	chr8(+):107293470-107379907	Nfat5	protein_coding

17321307	chr15(-):98663421-98677461	Rnd1	protein_coding
17473985	chr7(+):15692101-15693156	NA	NA
17376541	chr2(+):131909928-131938431	Prnd	protein_coding
17544786	chrX(-):136954988-136976874	Tmsb15b1	protein_coding
17464706	chr6(-):6877805-6882085	Dlx5	protein_coding
17491378	chr7(-):48866429-48881596	E2f8	protein_coding
17400250	chr3(+):95160457-95174024	Sema6c	protein_coding
17522876	chr9(+):118478189-118486132	Eomes	protein_coding
17322113	chr15(-):101996711-102004342	Krt8	protein_coding
17297750	chr14(+):25694170-25700468	Ppif	protein_coding
17537895	chrX(+):136270253-136271978	Ngfrap1	protein_coding
17319607	chr15(-):82329532-82338826	Naga	protein_coding
17484454	chr7(+):139943789-139945112	Utf1	protein_coding
17535353	chrX(+):71663667-71669257	Gpr50	protein_coding
17536969	chrX(+):103414467-103424583	Tsx	protein_coding
17447610	chr5(-):37820485-37824585	Msx1	protein_coding
17380766	chr2(+):180456245-180474867	Slco4a1	protein_coding
17396492	chr3(+):28781311-28798846	Eif5a2	protein_coding
17359088	chr19(+):37697808-37701536	Cyp26a1	protein_coding
17544689	chrX(-):135844275-135844731	Gprasp2	protein_coding
17251500	chr11(+):69059775-69061576	9330160F10Rik	protein_coding
17458592	chr6(+):52156902-52162289	Gm15051	processed_transcript
17330905	chr16(-):50719297-50732773	5330426P16Rik	protein_coding
17448712	chr5(-):72755718-72868459	Tec	protein_coding
17512086	chr8(-):95756950-95757084	SNORA76	snoRNA
17456131	chr6(+):17065149-17105828	Tes	protein_coding
17321474	chr15(-):98949841-98953551	Tuba1a	protein_coding

60

17536428	chrX(+):97072596-97082104	Pgr15l	protein_coding
17231694	chr10(+):13090691-13131694	Plagl1	protein_coding
17232912	chr10(+):41810574-41908436	Sesn1	protein_coding
17427312	chr4(-):95049034-95052222	Jun	protein_coding
17276814	chr12(+):80108034-80113000	Zfp36l1	protein_coding
17315718	chr15(-):5206661-5244187	Ptger4	protein_coding
17537839	chrX(+):135834109-135844731	Gprasp2	protein_coding
17536848	chrX(+):101794592-101798644	8030474K03Rik	protein_coding
17432488	chr4(-):143894237-143900380	Pramef6	protein_coding
17389456	chr2(-):113500679-113504034	Gm13964	processed_transcript
17340609	chr17(-):6738041-6782784	Ezr	protein_coding
17437558	chr5(+):57718021-58132240	Pcdh7	protein_coding
17429954	chr4(-):126150602-126163491	1700029G01Rik	protein_coding
17415323	chr4(+):88784963-88786518	Gm13276	pseudogene
17451816	chr5(-):116408491-116422864	Hspb8	protein_coding
17415333	chr4(+):88790805-88792360	Gm13276	pseudogene
17379224	chr2(+):163122606-163144267	Gm11454	processed_transcript

Table 3.2. Genes not zygotically activated, but whose expression is up-regulated following inhibition of the maturation-associated increase in SIN3A.

Annotation			
ID	SPOT ID	Gene name	Biotype
17270727	chr11(-):106126336-106127351	Gm11672	processed transcript
17297591	chr14(+):21263624-21263859	7SK	misc_RNA
17318403	chr15(-):76214101-76214205	U6	snRNA
17231033	chr1(-):191170296-191183340	Atf3	protein_coding
17240606	chr10(-):43583783-43584264	Cd24a	protein_coding
17400000	chr3(+):93555080-93564645	S100a10	protein_coding
17335788	chr17(+):31059604-31059731	5S_rRNA	rRNA
17312278	chr15(+):75759859-75759989	SNORA17	snoRNA
17250517	chr11(+):60804578-60804703	SNORA25	snoRNA
17287245	chr13(+):49714119-49714240	SNORA24	snoRNA
17249962	chr11(+):58126068-58128512	Gm12246	processed transcript
17356427	chr19(+):5447698-5455945	Fosl1	protein_coding
17270999	chr11(-):106783171-106783271	Ddx5	protein_coding
17374792	chr2(+):119325784-119335962	Dll4	protein_coding
17458514	chr6(+):49822710-49829507	Npy	protein_coding
17431478	chr4(-):135541888-135573630	Grhl3	protein_coding
17253832	chr11(+):79704630-79705420	Gm11205	processed transcript
17275015	chr12(+):35992907-36004087	Agr2	protein_coding
17327038	chr16(+):91372783-91405589	NA	NA
17506697	chr8(+):123653929-123663884	Rhou	protein_coding
17282776	chr12(-):86880703-86884814	6430527G18Rik	protein_coding
17500535	chr8(+):34807297-34819894	Dusp4	protein_coding
17391233	chr2(-):127138769-127143457	Itpripl1	protein_coding

17276139	chr12(+):71309884-71320107	Dact1	protein_coding
17366812	chr2(+):10489410-10489533	AL772216.12	miRNA
17366848	chr2(+):10496791-10496914	AL772216.12	miRNA
17333121	chr17(+):8434423-8442496	T	protein_coding
17336494	chr17(+):34263209-34269418	H2-Ab1	protein_coding
17439511	chr5(+):98180869-98187448	Prdm8	protein_coding
17335818	chr17(+):31295483-31350709	Slc37a1	protein_coding
17225191	chr1(-):86666291-86670573	Nppc	protein_coding
17439184	chr5(+):93267257-93276231	Ccng2	protein_coding
17274184	chr12(+):14494561-14495157	Gm9847	protein_coding
17366788	chr2(+):10484490-10484613	AL772216.36	miRNA
17366824	chr2(+):10491860-10491983	AL772216.36	miRNA
17402181	chr3(+):121723537-121735052	F3	protein_coding
17464549	chr6(-):3685677-3764713	Calcr	protein_coding
17250322	chr11(+):59921499-59921889	1810063I02Rik	processed transcript
17292507	chr13(-):49976258-49976488	Gm17611	protein_coding
17274959	chr12(+):33957671-33959831	Twist1	protein_coding
17223848	chr1(-):65100389-65103373	Cryga	protein_coding
17415310	chr4(+):88776176-88777731	Gm13276	pseudogene
17540374	chrX(-):15896663-15896769	U6	snRNA
17216402	chr1(+):106861173-106883348	Serpinb5	protein_coding
17233357	chr10(+):57486385-57513143	Hsf2	protein_coding
17286703	chr13(+):40727808-40735145	Gm16989	lincRNA
17225224	chr1(-):87147655-87156521	Ecel1	protein_coding
17366644	chr2(+):9877256-9878869	Gm13256	processed transcript
17364521	chr19(-):40550257-40588463	Aldh18a1	protein_coding

17272857	chr11(-):119077571-119086237	Cbx4	protein_coding
17415305	chr4(+):88773248-88774803	Gm13276	pseudogene
17281885	chr12(-):73100259-73113414	Six4	protein_coding
17422443	chr4(+):154960923-154962371	Hes5	protein_coding
17282216	chr12(-):80107760-80113013	Zfp36l1	protein_coding
17253133	chr11(+):76179671-76214827	Fam57a	protein_coding
17395499	chr2(-):180099465-180104488	Gm17180	processed transcript
17286295	chr13(+):30749226-30766927	Irf4	protein_coding
17366790	chr2(+):10485051-10485176	AL772216.29	miRNA
17233920	chr10(+):63382443-63408840	Dnajc12	protein_coding
17296896	chr14(+):4860406-5021482	Gm3242	pseudogene
17268137	chr11(-):95044474-95076801	Itga3	protein_coding
17454995	chr5(-):144735915-144761649	Tmem130	protein_coding
17464718	chr6(-):7675169-7693254	Asns	protein_coding
17500097	chr8(+):25017211-25023260	Tm2d2	protein_coding
17288836	chr13(+):77676821-77676951	SNORA17	snoRNA
17487422	chr7(-):19756131-19771016	Bcam	protein_coding
17407903	chr3(-):95796699-95796884	U1	snRNA
17379887	chr2(+):167248317-167248578	Gm17544	protein_coding
17279011	chr12(+):110841029-110843804	4921507G05Rik	lincRNA
17525578	chr9(-):37229149-37255738	Slc37a2	protein_coding
17281337	chr12(-):57540631-57546121	Foxa1	protein_coding
17519967	chr9(+):85842380-85847055	Tpbg	protein_coding
17373943	chr2(+):105668896-105703160	Pax6	protein_coding
17366687	chr2(+):10370451-10595253	Sfmbt2	protein_coding
17504293	chr8(+):95352268-95374293	Mmp15	protein_coding

17288057	chr13(+):62136762-62136831	SNORA32	snoRNA
17293515	chr13(-):62543434-62543503	SNORA32	snoRNA
17356383	chr19(+):5298331-5308739	Gal3st3	protein_coding
17308881	chr14(-):79288749-79301635	1190002H23Rik	protein_coding
17541383	chrX(-):48171969-48208878	Zdhhc9	protein_coding
17336921	chr17(+):35065388-35070050	Ly6g6c	protein_coding
17515436	chr9(+):22411577-22444681	9530077C05Rik	protein_coding
17409154	chr3(-):108012250-108017973	Gstm1	protein_coding
17232853	chr10(+):41476314-41487032	Mical1	protein_coding
17217440	chr1(+):134405781-134411740	Cyb5r1	protein_coding
17375503	chr2(+):122636986-122641191	AA467197	protein_coding
17520315	chr9(+):92250057-92272561	Plscr1	protein_coding
17445236	chr5(+):150708044-150708149	U6	snRNA
17450366	chr5(-):103989762-104021919	Hsd17b11	protein_coding
17489905	chr7(-):38220654-38227994	Plekhf1	protein_coding
17351485	chr18(+):67641599-67654162	Psmg2	protein_coding
17344124	chr17(-):34952240-34952309	1110038B12Rik	processed transcript
17277622	chr12(+):87332488-87335655	Gm17256	lincRNA
17374738	chr2(+):119167773-119172390	Gchfr	protein_coding
17302598	chr14(+):110970788-110971471	Gm6280	protein_coding
17483565	chr7(+):127983079-127985701	B230325K18Rik	protein_coding
17231855	chr10(+):19356539-19358606	Olig3	protein_coding
17257937	chr11(+):111066164-111076825	Kcnj2	protein_coding

Table 3.3. qRT- PCR confirmation of four transcripts from each class whose expression was increased following inhibition of the maturation-associated increase in SIN3A.

Probe	Sample	CT1	CT2	Mean CT	DCT	DDCT	Fold change
Atf3	control	34.13	34.06	34.10	10.09	0.00	**1.00**
	Sin3a KD	32.00	32.16	32.08	8.04	-2.05	**4.13**
Calcr	control	36.00	36.27	36.14	12.13	0.00	**1.00**
	Sin3a KD	37.39	36.88	37.14	13.10	0.97	**0.51**
Cd24a	control	35.00	34.93	34.97	10.96	0.00	**1.00**
	Sin3a KD	34.93	34.54	34.74	10.70	-0.26	**1.20**
Crabp1	control	33.00	32.52	31.24	7.23	0.00	**1.00**
	Sin3a KD	30.82	30.79	30.81	6.77	-0.47	**1.38**
Hsd17b11	control	36.85	37.42	37.14	13.13	0.00	**1.00**
	Sin3a KD	36.00	36.05	36.03	11.99	-1.14	**2.20**
Krt18	control	33.57	33.62	33.60	9.59	0.00	**1.00**
	Sin3a KD	32.23	32.00	32.12	8.08	-1.51	**2.85**
Osr2	control	35.00	35.22	35.11	11.10	0.00	**1.00**
	Sin3a KD	32.90	33.27	33.09	9.05	-2.06	**4.16**
Rgs16	control	33.23	33.00	33.12	9.11	0.00	**1.00**
	Sin3a KD	31.93	31.64	31.79	7.75	-1.36	**2.57**
H2a	control	24.02	24.00	24.01			
	Sin3a KD	24.10	23.98	24.04			

3.2 Discussion

During early mouse development, a highly differentiated female germ cell, the oocyte, transforms into a zygote, which is the source of the undifferentiated totipotent blastomeres. Surprisingly, this biological switch occurs during a transcriptionally inactive period; therefore, this transformation must rely on the transcripts bestowed to the zygote by the mother (the oocyte) until the zygotic genome is activated. During this transition from maternal to zygotic control of cellular functions, the major ZGA promotes a dramatic change of global gene expression (Hamatani et al., 2004) that is essential for continued development beyond the 2-cell stage. Superimposed on ZGA and reprogramming is the formation of a chromatin-mediated transcriptionally repressive state that promotes the repression of endogenous genes during the 2-cell stage (Wiekowski et al., 1991; Majumder et al., 1993; Davis et al., 1996). This transcriptionally repressive state is relieved when global histone hyperacetylation is induced (Wiekowski et al., 1991; Davis et al., 1996). Although the genes that are reprogrammed have been identified, a major unresolved problem is how this reprogramming of global gene expression occurs through the utilization of a maternally-derived transcription machinery.

Several modes of regulation may be responsible for ZGA and the subsequent reprogramming of global gene expression with a maternally-derived transcription machinery in early mouse development. One locus of regulation may be at the level of RNA polymerase II, particularly the post-translational changes affecting this enzyme. Phosphorylation of RPB1, most likely by MAP kinase, occurs in mouse oocytes; the phosphorylation may destabilize the holoenzyme and be responsible for the global transcriptional silencing observed in these cells, which is continued into the 1-cell stage of mouse preimplantation development (Wei et al., 2015; Abe et al., 2010). Because the amount of the hyperphosphorylated form of RPB1 decreases rapidly following fertilization when the enzyme responsible for the enzyme's phosphorylation is inactive in *Xenopus*

(Bellier et al., 1997), CTD phosphatases may counteract the action of MAP kinase, leading to dephosphorylation of the hyperphosphorylated form of RPB1 in mouse 1-cell embryos and activation of zygotic transcription.

Changing the composition of the chromatin such as the elimination of maternal histone variants associated with transcriptional repression may be responsible for the global transcriptional activation and subsequent reprogramming of gene expression in mouse embryos. Several histone variants associated with transcriptional repression are lost following fertilization. For example, the maternal histone variant macroH2A, which is a core histone related to canonical histone H2A (Pehrson and Fried, 1992), is generally involved with transcriptionally repression due to its association with condensed chromatin such as inactive genes and the inactive X chromosome (Buschbeck et al., 2009; Costanzi and Pehrson, 1998). During ES cell differetiation and in development, macroH2A is deposited at pluripotency genes and can act as an epigenetic barrier during the process of somatic cell reprogramming (Gaspar-Maia et al., 2013). Interestingly, in developing and maturing mouse oocytes, macroH2A is associated with chromosomes and is lost from the embryo following fertilization, specifically by the late 2 pronuclei stage (Chang et al., 2005). MarcroH2A does not reappear until after the 8-cell stage, and its expression persists in the morula and blastocysts, which is the stage at which the first cellular differentiation event occurs during development.

Another elegant, but simple solution to promote the success of reprogramming gene expression is the translational recruitment of dormant maternal mRNAs that encode for chromatin-modifying-related factors during oocyte maturation and following fertilization in the mouse. These critical factors will rearrange the chromatin structure of the early embryo, and subsequently alter RNA polymerase II promoter accessibility to elicit transcription and the subsequent reprogramming of global gene expression. By utilizing the recruitment of dormant maternal mRNAs for translation during oocyte maturation, the oocyte is able to utilize a mechanism to synthesize a new functional protein

product at the appropriate developmental time without new transcription.

The mechanism for the translational recruitment of dormant maternal mRNAs is well understood in oocytes (Groppo and Richter, 2009). In general, many dormant but stable mRNAs that have a relatively short poly (A) tail in the oocyte are inhibited from translation by sequence-specific RNA binding proteins such as Maskin, which affects translational initiation. In particular, Maskin, which interacts with CPE-containing mRNAs that are bound by CPEB, weakly interacts with eukaryotic translation initiation factor 4E (eIF4E) and prevents its interaction with eIF4G and leads to translational repression (Stebbins-Boaz et al., 1999). When the oocyte resumes meiosis, the bound CPEB stimulates the elongation of the poly (A) tail, which then binds poly(A) binding protein (PABP). PABP then associates with eIF4G and helps disrupt the Maskin-eIF4E interaction to allow for the translational activation of the CPE-containing mRNAs (Richter and Sonenberg, 2005). The dissociation of Maskin from eIF4E and translational activation is also mediated by several CDK1 driven phosphorylation events of Maskin (Barnard et al., 2005).

Previously, the identification of the dormant maternal mRNAs that undergo translational recruitment following oocyte maturation was serendipitous. For example, *c-mos*, a MAPK pathway activator, was serendipitously identified as a dormant maternal transcript that is recruited for translation during oocyte maturation. The translational recruitment of this transcript is needed to maintain cellular arrest at metaphase II (Colledge et al., 1994; Sheets et al. 1995; Sagata, 1997). However, these dormant maternal mRNAs are now being identified on a global scale by using previously generated data from microarray experiments in which oligo(dT) primers were used to generate cDNA from mouse oocytes and embryos (Zeng et al., 2004). The elongation of the poly (A) tail that is associated with translational activation provides for a more efficient oligo(dT) priming of RNA isolated from the mouse oocytes and embryos. The increased priming efficiency associated with oligo(dT) primers results in an increase in the relative abundance of the transcript in 1-cell embryos when compared to full-grown GV-intact

69

oocytes.

 After analyzing the microarray data, many transcripts displayed an increase in relative abundance between the full-grown GV-intact oocyte and 1-cell stage, and some of these potential dormant maternal transcripts that are recruited for translation during oocyte maturation and/or following fertilization encode for chromatin-modifying-related factors (Zeng et al., 2004). A few such transcripts were *Sin3a,* a chromatin remodeler (Bansal et al., 2016)*, Rbbp7,* a core histone biding protein (Verreault et al., 1998), and *Ezh2,* a histone H3K27 methyltransferase (Cao and Zhang, 2004)*.* A prominent characteristic of these potentially translationally recruited transcripts is their raw score for their relative abundance is high when compared to the value of the normalized chip. This high abundance of the translationally recruited maternal transcript provides a strategy for the oocyte to synthesize a large amount of protein during a short period of time before the function of the protein is needed. The following work focuses on *Sin3a* because SIN3A is essential for mouse development (Cowley et al., 2005; Dannenberg et al., 2005) and present in a HDAC-containing complex (Bansal et al., 2016), which have a role in the formation of the transcriptionally repressive state that develops during ZGA and the reprogramming of gene expression (Ma and Schultz, 2008).

 During oocyte maturation and following fertilization, elements in the 3' UTR, such as the cytoplasmic polyadenylation element (CPE, $U_{4-5}A_{1-2}U$), polyuridine stretch and polyadenylation signal sequence (AAUAAA), control the translation of certain maternal mRNAs by elongating the poly (A) tail (Fox et al., 1990; Oh et al., 2000). After searching the 3' UTR of *Sin3a* transcript for these elements, a potential CPE (U_5AU) and a polyuridine stretch (U_{13}) are present within ~210 nucleotides and directly preceding the polyadenylation signal sequence. These elements may contribute to the increase in the amount of SIN3A protein observed during oocyte maturation and following fertilization by directing the polyadenylation of the *Sin3a* transcript that will lead to the translational activation of the transcript. Examination of microarray data of oligo

(dT) primed mouse oocyte and 1-cell embryo cDNA reveal an elevation in the relative abundance of *Sin3a* transcript between the full-grown GV-intact oocytes and 1-cell stages (Zeng et al., 2004). The elevation in the relative abundance of the *Sin3a* transcript likely reflects the polyadenylation of the transcript during oocyte maturation that leads to an increased priming efficiency of the oligo (dT) primer during reverse transcription since essentially no new transcription occurs between the two stages. These results are consistent with *Sin3a* mRNA being a dormant maternal mRNA that is recruited for translation during oocyte maturation and following fertilization. It would be interesting to mutate the CPE located within the 3' UTR of *Sin3a* mRNA to determine if it attenuates the maturation-associated increase in SIN3A, and the polyuridine stretch (U_{13}) to determine if the increase in maternal SIN3A following fertilization is impaired.

A more recent genome-wide profiling of polysome mRNA identified an enrichment of a motif for the RNA-binding protein deleted in azoospermia-like (DAZL) along with the CPE motif within the 3' UTR of mRNAs recruited to the polysomes during mouse oocyte maturation (Chen et al., 2011). Although DAZL has been proposed to function as a translational activator, there is evidence supporting it as a translation repressor in full-grown GV-intact oocytes. Interestingly, the 3' UTR of *Sin3a* mRNA contains several putative DAZL elements within 200 nucleotides of the polyadenylation signal sequence. It would be interesting to determine if these motifs have a role in the translational recruitment of the *Sin3a* transcript to the polysomes during oocyte maturation and/or the translational repression of the *Sin3a* transcript in mouse oocytes.

The restricted presence of the maturation-associated increase in SIN3A protein mainly to the 1-cell stage likely constrains its function to this short window of mouse preimplantation development. Because there was a relatively significant amount of *Sin3a* transcript present at the 2-cell stage and maternal SIN3A degradation was substantially inhibited by a proteasome inhibitor, the dramatic reduction of maternal SIN3A to nearly undetectable levels by the 2-cell stage suggest that the protein loss is likely a result of proteasome-mediated

71

degradation rather than the decrease in the relative abundance of *Sin3a* mRNA between the MII and 2-cell stages. The low SIN3A protein levels can also result from a decrease in protein synthesis of SIN3A. If the loss in the increase in maternal SIN3A protein is mainly due to degradation, it leads to an emerging question as to which pathway is involved in the degradation of maternal SIN3A protein: ubiquitin-dependent or ubiquitin-independent proteasomal degradation. If maternal SIN3A undergoes clearance via the ubiquitin-independent proteasomal degradation pathway, it would be interesting to determine what mechanism is in place to protect maternal SIN3A from degradation to allow proper protein accumulation between the MII and 1-cell stages. It may be that assembly of SIN3A into the SIN3A-co-repressor complex protects SIN3A from 20S proteasomal degradation, as seen when CDK inhibitor p21 (WAF1/CIP1) binds directly to cyclin D1 (Touitou et al., 2001; Coleman et al., 2003). It is possible that a post-translational modification occurs following ZGA that dissociates SIN3A from the complex, and allows for it to be degraded by the proteasome.

Because the function of maternal SIN3A may be limited to a short window of mouse preimplantation development and the epigenetic modifications of the paternal and maternal genomes are distinct at fertilization and during the 1-cell stage (Santos et al., 2005; Erhardt et al., 2003; Lepikhov and Walter, 2004; Liu et al., 2004), I focused my analysis mostly on determining the effects of depleting maternal SIN3A in 1-cell embryos that were derived from MII eggs fertilized in vitro. Although maternal SIN3A appears equally distributed to both pronuclei in the 1-cell mouse embryo, differences in chromatin-association of nuclear proteins at this stage is know to exist. For example, PGC7/STELLA appears in both pronuclei at the 1-cell stage, but has a weak association to the paternal genome (Nakamura et al., 2012). However, no difference in the chromatin-association of maternal SIN3A was observed between the maternal and paternal pronuclei when 1-cell embryos were permeabilized prior to fixation. Any difference in localized gene occupancy between the maternal and paternal remains unknown

and can only be addressed once chromatin immunoprecipitation assays allow for small cell numbers to be analyzed.

The HDAC inhibitor TSA led to histone hyperacetylation, whereas blocking the maturation-associated increase in maternal SIN3A surprisingly results in no histone hyperacetylation. Rather, histone hypoacetylation is seen in the 1-cell embryos depleted of maternal SIN3A. Although a decrease in nuclear HDAC2 was seen in *Sin3a* null oocytes, the amount of nuclear HDAC1 remained unchanged (Ma et al., 2015). Because removal of HDAC1, but not HDAC2 in preimplantation embryos leads to global histone hyperacetylation (Ma et al., 2008), a likely decrease in nuclear HDAC2 when the maturation-associated increase in maternal SIN3A is inhibited will not likely effect the global histone acetylation state of 1-cell mouse embryos. However, as seen with oocytes, the amount of nuclear HDAC1 likely remains unchanged in 1-cell embryos depleted of maternal SIN3A, and therefore would still be present and able to function in 1-cell embryos. Because the SIN3A-co-repressor complex is a major HDAC1 and HDAC2 containing complex and SIN3A is an essential component of the multi-subunit complex, depleting maternal SIN3A may likely allow HDAC1 and the decreased nuclear amount of HDAC2 to associate with other HDAC1/2-containing complexes. If the other HDAC1/2-containing complexes have greater enzymatic activity than the SIN3A-co-repressor complex, then the observed histone hypoacetylation could likely occur.

The observed histone hypoacetylation and depletion of maternal SIN3A in mouse 1-cell embryos had no effect on global transcription in the zygote, however, the histone hypoacetylation could account for the 50% reduction in global transcription observed in the 2-cell embryos depleted of maternal SIN3A because of the known links between transcription and the histone modifications that are affected in these embryos. For example, the enrichment of H4K12ac in transcribed regions, which was globally decreased in the maternal SIN3A-depleted embryos, is associated with transcriptional elongation (Cho et al., 1998) and could contribute to the reduced global transcription at the 2-cell stage.

Furthermore, the hypoacetylation of H4K8ac, which is enriched in the promoter and body of transcribed genes and linked to transcriptional activation (Wang et al., 2008), and H3K18ac, which is enriched around the transcription start site and may be important for recruiting Pol II to target genes to initiate transcription (Jin et al., 2011), could also contribute to the decreased global transcription.

Blocking the maturation-associated increase in maternal SIN3A led to a developmental arrest at the 2-cell stage. The function of only a few other genes (*Mater*, *mHR6A, Trim24*, and *Brg1*) has been identified as being required for embryonic development beyond the 2-cell stage as *Sin3a* (Tong et al., 2000; Roest et al., 2004; Torres-Padilla and Zernicka-Goetz, 2006; Bultman et al., 2006). Failure to activate the zygotic genome or successfully reprogram the pattern of gene expression that accompanies ZGA is a source for the developmental arrest. The expression of a restricted subset of genes that are normally and not normally activated during ZGA and reprogramming of gene expression in maternally depleted SIN3A 2-cell embryos likely underlines the observed 2-cell arrest. The observation that only a restricted subset of genes that are normally activated during ZGA are misexpressed is consistent with SIN3A co-repressor complex being one of several HDAC1/2-containing complexes that may have a role in the repression of genes during the formation of the global transcriptionally repressive state that develops during ZGA.

Analysis of the misexpressed genes in maternal SIN3A-depleted embryos was uninformative in providing a framework for understanding the mechanistic relationship between the depletion of maternally derived SIN3A co-repressor complex and relief of repression of a restricted subset of genes. Mapping of the misexpressed genes to chromosomes did not reveal unexpected gene clusters, and the misexpressed genes represented multiple classes of genes and did not solely represent one gene class (e.g., noncoding RNAs). However, the analysis of the misexpressed genes revealed that a bivalent promoter, which carry both H3K4me3 an H3K27me3 in mouse embryonic stem cells, marked about 40 genes whose expression was increased in SIN3A maternally depleted 2-cell

embryos. It would be interesting to determine whether the bivalent chromatin mark is present at the promoters of these genes in 2-cell mouse embryos and observe how they change over the course of preimplantation development. Investigating whether one or both of these histone modifications are needed for the recruitment of the SIN3A-co-repression complex to these genes should facilitate the development of a working model outlining the linkage between the maternal SIN3A-co-repression complex and the reprogramming of gene expression. However, these questions could only be addressed once chromatin immunoprecipitation assays allow for small cell numbers because of the excessive amount of time and effort needed to generate the biological samples that were used in this study.

The experiment where elevated levels of maternal SIN3A was maintained beyond the time when it normally decreases to undetectable levels yields insights beyond what I was expecting to discover. Analysis of the control embryos suggest that development to the blastocyst stage depends on the control cRNA that is injected and highlights the need to be cautious about choosing a proper control in the experiment. We observed that *mCherry* cRNA is detrimental to blastocyst developmental while *Luc* cRNA and buffer had no effect. The overexpression experiment was unsuccessful because of the rapid loss of the exogenously expressed SIN3A, a finding consistent with the endogenous maternal SIN3A. In order to assess whether the rapid loss of maternal SIN3A is essential for mouse preimplantation development, identifying and then mutating the amino acid sequences responsible for the rapid turnover of (e.g., of destruction box) (Glotzer et al., 1991) SIN3A may allow for such a study to be conducted.

In summary, the presented data provide a role for SIN3A co-repressor complex, an HDAC-containing complex, in the development of the transcriptionally repressive state during mouse preimplantation development. In this model, SIN3A is encoded by a dormant maternal mRNA that is recruited for translation during oocyte maturation and following fertilization. Blocking the

recruitment of maternal *Sin3a* mRNA impairs the expression of a subset of zygotically and non-zygotically activated genes during the establishment of the transcriptionally repressive state that is superimposed on ZGA. These results provide a unique approach with which to study the reprogramming of gene expression during preimplantation development and leads to a number of additional questions requiring further research. It would certainly be interesting to determine the precise mechanism between the loss of maternal SIN3A and relief of repression of the genes misexpressed in maternal SIN3A-depleted embryos. Overall, the data implicate the role for the translational recruitment of dormant maternal mRNAs encoding chromatin remodelers like SIN3A as a post-transcriptional mechanism for how reprogramming of gene expression occurs utilizing a maternally-derived transcription machinery. Interestingly, what emerges from the analysis of the microarray data of oligo (dT) primed mouse oocyte and 1-cell embryo cDNAs is that the transcripts that show a relative increase in abundance between the full-grown GV-intact oocyte and 1-cell stage encode for proteins which are central to cellular processes that should either not function or function minimally in the oocyte but then are required by the 1-cell stage of development. For example, mRNAs are relatively stable during oocyte growth due to the RNA binding protein MSY2 (Yu et al., 2004). The mRNA degradation machinery during this period is minimally functional and the resumption of meiosis triggers a transition from maternal mRNA stability to instability, in which MSY2 becomes phosphorylated by CDC2A. This phosphorylation event makes maternal mRNAs more susceptible to the oocyte's RNA degradation machinery (Medvedev et al., 2008). DCP1A and DCP2, proteins responsible for decapping mRNA, are encoded by dormant maternal mRNAs that are recruited for translation during oocyte maturation. The increase in both these proteins ensures that the maternal mRNAs are stable in the oocyte but are unstable and degraded following oocyte maturation (Ma et al., 2013). Oocytes should not have the capacity to undergo a round of DNA replication, but need to replicate their DNA following fertilization. ORC6L and CDC6, critical

factors for assembly of a functional origin of replication complex, are encoded by dormant maternal mRNAs that are recruited for translation during oocyte maturation (Murai et al., 2010; Anger et al., 2005). The recruitment of these transcripts during oocyte maturation ensures that DNA replication does not occur in the oocyte but that the 1-cell embryos are capable of undergoing a round of DNA replication.   The active DNA demethylation event occurring solely on the paternal genome during the 1-cell stage of mouse development is mediated by TET3 (Iqbal et al., 2011; Gu et al., 2011; Wossidlo et al., 2011). Oocyte maturation and fertilization is accompanied by an increase in the protein synthesis of TET3 that results in loss of the paternal 5mC, and appearance of hydroxymethylcytosine (5hmC) (Inoue and Zhang, 2011). Inhibiting the increase in maternal TET3 using a siRNA approach results in the inhibition of the oxidation of 5mC to 5hmC, and surprisingly, the loss of maternal TET3 had no effect on ZGA or transposable element activation (Inoue et al., 2012). The increase in TET3 ensures the 1-cell embryo, but not the oocyte, undergoes active DNA demethylation following fertilization.

A similar conclusion emerged when a different approach was undertaken to determine, at a global scale, which maternal mRNAs are recruited for translation during oocyte maturation. Results from genome-wide analysis of transcripts that were recruited to polysomes during mouse oocyte maturation revealed that these transcripts encode for well-established regulators of the cell cycle, like components of the spindle assembly checkpoint (*Mad2* and *Bub1b*) and the anaphase-promoting complex (*Apc1, Apc10*) (Chen et al., 2011). Interestingly, the processes that are encoded for by the transcripts recruited to the polysomes are not limited to regulators of cell cycle, but include chromatin remodelers and transcription regulators, which is consistent with my findings from the microarray data. The coordinated translational recruitment of specific maternal mRNAs during oocyte maturation and following fertilization is a mechanism the oocyte utilizes and is likely essential for the critical events that take place during the initial stages of embryo development until transcription is

activated and the embryo assumes control of development.

REFERENCES

Abe, K., Inoue, A., Suzuki, M.G., and Aoki, F. (2010). Global gene silencing is caused by the dissociation of RNA polymerase II from DNA in mouse oocytes. J Reprod Dev *56*, 501-507.

Abe, K., Yamamoto, R., Franke, V., Cao, M., Suzuki, Y., Suzuki, M.G., Vlahovicek, K., Svoboda, P., Schultz, R.M., and Aoki, F. (2015). The first murine zygotic transcription is promiscuous and uncoupled from splicing and 3' processing. EMBO J *34*, 1523-1537.

Adenot, P.G., Mercier, Y., Renard, J.P. and Thompson, E.M. (1997). Differential H4 acetylation of paternal and maternal chromatin precedes DNA replication and differential transcriptional activity in pronuclei of 1-cell mouse embryos. Development *124*, 4625-4625.

Anger, M., Stein, P., and Schultz, R.M. (2005). CDC6 requirement for spindle formation during maturation of mouse oocytes. Biol Reprod *72*, 188-194.

Aoki, F., Worrad, D.M., and Schultz, R.M. (1997). Regulation of transcriptional activity during the first and second cell cycles in the preimplantation mouse embryo. Dev Biol *181*, 296-307.

Araki K., Naito K., Haraguchi S., Suzuki R., Yokoyama M., Inoue M., Aizawa S., Toyoda Y., and Sato E. (1996). Meiotic abnormalities of *c-mos* knock- out mouse oocytes: activation after first meiosis or entrance into third meiotic metaphase. Biol Reprod *55*, 1315-1324.

Ayer, D.E., Lawrence, Q.A., and Eisenman, R.N. (1995). Mad-Max transcriptional repression is mediated by ternary complex formation with mammalian homologs of yeast repressor Sin3. Cell *80*, 767-776.

Baltus, G.A., Kowalski, M.P., Tutter, A.V., and Kadam, S. (2009a). A positive regulatory role for the mSin3A-HDAC complex in pluripotency through Nanog and Sox2. J Biol Chem *284*, 6998-7006.

Baltus, G.A., Kowalski, M.P., Zhai, H., Tutter, A.V., Quinn, D., Wall, D., and Kadam, S. (2009b). Acetylation of sox2 induces its nuclear export in embryonic stem cells. Stem Cells *27*, 2175-2184.

Bansal, N., David, G., Farias, E., and Waxman, S. (2016). Emerging Roles of Epigenetic Regulator Sin3 in Cancer. Adv Cancer Res *130*, 113-135.

Bansal, N., Petrie, K., Christova, R., Chung, C. Y., Leibovitch, B. A., Howell, L., et al. (2015). Targeting the SIN3A-PF1 interaction inhibits epithelial to

mesenchymal transition and maintenance of a stem cell phenotype in triple negative breast cancer. Oncotarget *6*, 34087-34105.

Barnard, D.C., Cao, Q., and Richter, J.D. (2005). Differential phosphorylation controls Maskin association with eukaryotic translation initiation factor 4E and localization on the mitotic apparatus. Mol Cell Biol *25*, 7605-7615.

Beaujean, N., Hartshorne, G., Cavilla, J., Taylor, J., Gardner, J.,Wilmut, I., Meehan, R. and Young, L. (2004). Non-conservation of mammalian preimplantation methylation dynamics. Curr Biol *14*, R266-R267.

Bellier, S., Dubois, M.F., Nishida, E., Almouzni, G., and Bensaude, O. (1997). Phosphorylation of the RNA polymerase II largest subunit during Xenopus laevis oocyte maturation. Mol Cell Biol *17*, 1434-1440.

Bolton, V.N., Oades, P.J., and Johnson, M.H. (1984). The relationship between cleavage, DNA replication, and gene expression in the mouse 2-cell embryos. J Embryol Exp Morphol *79*, 139-163.

Bouniol-Baly, C., Hamraoui, L., Guibert, J., Beaujean, N., Szöllösi, M.S., and Pascale Debey, P. (1999). Differential transcriptional activity associated with chromatin configuration in fully grown mouse germinal vesicle oocytes. Biol Reprod *60*, 580-587.

Bultman, S.J., Gebuhr, T.C., Pan, H., Svoboda, P., Schultz, R.M., and Magnuson, T. (2006). Maternal BRG1 regulates zygotic genome activation in the mouse. Genes Dev *20*, 1744-1754.

Burns, K.H., Viveiros, M.M., Ren, Y., Wang, P., DeMayo, F.J., Frail, D.E., Eppig, J.J., and Matzuk, M.M. (2003). Roles of NPM2 in chromatin and nucleolar organization in oocytes and embryos. Science *300*, 633-636.

Buschbeck, M., Uribesalgo, I., Wibowo, I., Rué, P., Martin, D., Gutierrez, A., Morey, L., Guigó, R., López-Schier, H., Di Croce, L. (2009). The histone variant macroH2A is an epigenetic regulator of key developmental genes. Nat Struct Mol Biol *16*, 1074-1079.

Cao, R., and Zhang, Y. (2004). The functions of E(Z)/EZH2-mediated methylation of lysine 27 in histone H3. Curr Opin Genet Dev *14*, 155-164.

Carvalho, B.S., and Irizarry, R.A. (2010). A framework for oligonucleotide microarray preprocessing. Bioinformatics *26*, 2363-2367.

Chang, C.C., Ma, Y., Jacobs, S., Tian, X.C., Yang, X., and Rasmussen, T.P. (2005). A maternal store of macroH2A is removed from pronuclei prior to onset of somatic macroH2A expression in preimplantation embryos. Dev Biol *278*, 367-

380.

Chatot, C.L., Ziomek, C.A., Bavister, B.D., Lewis, J.L., and Torres, I. (1989). An improved culture medium supports development of random-bred 1-cell mouse embryos in vitro. J Reprod Fertil *86*, 679-688.

Chen, J., Melton, C., Suh, N., Oh, J. S., Horner, K., Xie, F., et al. (2011). Genome-wide analysis of translation reveals a critical role for deleted in azoospermia-like (Dazl) at the oocyte-to-zygote transition. Genes and Dev *25*, 755-766.

Cho, H., Orphanides, G., Sun, X., Yang, X.J., Ogryzko, V., Lees, E., Nakatani, Y., and Reinberg, D. (1998). A human RNA polymerase II complex containing factors that modify chromatin structure. Mol Cell Biol *18*, 5355-5363.

Choi, E., Han, C., Park, I., Lee, B., Jin, S., Choi, H., Kim Do, H., Park, Z.Y., Eddy, E.M., and Cho, C. (2008). A novel germ cell-specific protein, SHIP1, forms a complex with chromatin remodeling activity during spermatogenesis. J Biol Chem *283*, 35283-35294.

Coleman, M.L., Marshall, C.J., and Olson, M.F. (2003). Ras promotes p21(Waf1/Cip1) protein stability via a cyclin D1-imposed block in proteasome-mediated degradation. EMBO J *22*, 2036-2046.

Colledge, W.H., Carlton, M.B., Udy, G.B., and Evans, M.J. (1994). Disruption of c-mos causes parthenogenetic development of unfertilized mouse eggs. Nature *370*, 65-68.

Costanzi, C., and Pehrson, J. (1998). Histone macroH2A1 is concentrated in the inactive X chromosome of female mammals. Nature *393*, 599-601.

Cowley, S.M., Iritani, B.M., Mendrysa, S.M., Xu, T., Cheng, P.F., Yada, J., Liggitt, H.D., and Eisenman, R.N. (2005). The mSin3A chromatin-modifying complex is essential for embryogenesis and T-cell development. Mol Cell Biol *25*, 6990-7004.

Dahmus, M.E. (1996). Reversible phosphorylation of the C-terminal domain of RNA polymerase II. J Biol Chem *271*, 19009-19012.

Dannenberg, J.H., David, G., Zhong, S., van der Torre, J., Wong, W.H., and Depinho, R.A. (2005). mSin3A corepressor regulates diverse transcriptional networks governing normal and neoplastic growth and survival. Genes Dev *19*, 1581-1595.

Davis, W., De Sousa, P.A., and Schultz, R.M. (1996). Transient expression of translation initiation factor eIF-4C during the 2-cell stage of the preimplantation

mouse embryo: identification by mRNA differential display and the role of DNA replication in zygotic gene activation. Dev Biol *174*, 190-201.

De La Fuente, R., Viveiros, M.M., Burns, K.H., Adashi, E.Y., Matzuk, M.M., and Eppig, J.J. (2004). Major chromatin remodeling in the germinal vesicle (GV) of mammalian oocytes is dispensable for global transcriptional silencing but required for centromeric heterochromatin function. Dev Biol *275*, 447-458.

Dean, W., Santos, F., Stojkovic, M., Zakhartchenko, V., Walter, J., Wolf, E. and Reik, W. (2001). Conservation of methylation reprogramming in mammalian development: aberrant reprogramming in cloned embryos. Proc Natl Acad Sci USA *98*, 13734-13738.

Debey, P., Szöllösi, M.S., Szöllösi, D., Vautier, D., Girousse, A. and Besombes, D. (1993). Competent mouse oocytes isolated from antral follicles exhibit different chromatin organization and follow different maturation dynamics. Mol Reprod Dev *36*, 59-74.

Denslow, S.A., and Wade, P.A. (2007). The human Mi-2/NuRD complex and gene regulation. Oncogene *26*, 5433-5438.

Downs, S.M., Coleman, D.L., and Eppig JJ. (1986). Maintenance of murine oocyte meiotic arrest: uptake and metabolism of hypoxanthine and adenosine by cumulus cell-enclosed and denuded oocytes. Dev Biol *117*, 174-183.

Endo, Y., Schultz, R.M., and Kopf, G.S. (1987). Effects of phorbol esters and a diacylglycerol on mouse eggs: inhibition of fertilization and modification of the zona pellucida. Dev Biol *119*, 199-209.

Eppig, J.J., Schultz, R.M., O'Brien, M., and Chesnel, F. (1994). Relationship between the developmental programs controlling nuclear and cytoplasmic maturation of mouse oocytes. Dev Biol *164*, 1-9.

Eppig, J.J. (1996). Coordination of nuclear and cytoplasmic oocyte maturation in eutherian mammals. Reprod Fertil Dev *8*, 485-489.

Eppig, J.J. and Schroeder, A.C. (1989). Capacity of mouse oocytes from preantral follicles to undergo embryogenesis and development to live young after growth, maturation and fertilization in vitro. Biol Reprod *41*, 268-276.

Eppig, J.J., and O'Brien, M.J. (1996). Development in vitro of mouse oocytes from primordial follicles. Biol Reprod 54, 197-207.

Erbach, G.T., Lawitts, J.A., Papaioannou, V.E., and Biggers, J.D. (1994). Differential growth of the mouse preimplantation embryo in chemically defined

media. Biol Reprod 50, 1027-1033.

Erhardt, S., Su, I.H., Schneider, R., Barton, S., Bannister, A.J., Perez-Burgos, L., Jenuwein, T., Kouzarides, T., Tarakhovsky, A. and Surani, M.A. (2003). Consequences of the depletion of zygotic and embryonic enhancer of zeste 2 during preimplantation mouse development. Development *130*, 4235-4248.

Flach, G., Johnson, M.H., Braude, P.R., Taylor, K.A.S. and Bolton, V.N. (1982). The transition from maternal to embryonic control in the 2-cell mouse embryo. EMBO J *1*, 681-686.

Fleming, T.P, Sheth, B., and Fresenko, I. (2001). Cell adhesion in the pre implantation mammalian embryo and its role in trophectoderm differentiation and blastocysts morphogenesis. Front Biosci *6*, D1000- D1007.

Fox, C.A., and Wickens, M. (1990). Poly(A) removal during oocyte maturation: a default reaction selectively prevented by specific sequences in the 3' UTR of certain maternal mRnAs. Genes Dev *4*, 2287-2298.

Fulka, H., Mrazek, M., Tepla, O., and Fulka, J. Jr. (2004). DNA methylation pattern in human zygotes and developing embryos. Reproduction *128*, 703-708.

Gaspar-Maia, A., Qadeer, Z. A., Hasson, D., Ratnakumar, K., Leu, N. A., Leroy, G., et al. (2013). MacroH2A histone variants act as a barrier upon reprogramming towards pluripotency. Nat Commun *4*, 1565.

Gentleman, R.C., Carey, V.J., Bates, D.M., Bolstad, B., Dettling, M., Dudoit, S., Ellis, B., Gautier, L., Ge, Y., Gentry, J., Hornik, K., Hothorn, T., et al. (2004). Bioconductor: open software development for computational biology and bioinformatics. Genome Biol *5*, R80.

Glotzer, M., Murray, A.W., and Kirschner, M.W. (1991). Cyclin is degraded by the ubiquitin pathway. *Nature 349*, 132-138.

Groppo, R., and Richter, J.D. (2009). Translational control from head to tail. Curr Opin Cell Biol *21*, 444-451.

Gu, T.P., Guo, F., Yang, H., Wu, H.P., Xu, G.F., Liu, W., Xie, Z.G., Shi, L., He, X., Jin, S.G., et al. (2011). The role of Tet3 DNA dioxygenase in epigenetic reprogramming by oocytes. Nature *477*, 606-610.

Hamatani, T., Carter, M.G., Sharov, A.A., and Ko, M.S.H. (2004). Dynamics of global gene expression changes during mouse preimplantation development. Dev Cell *6*, 117-131.

Hassig, C.A., Fleischer, T.C., Billin, A.N., Schreiber, S.L., and Ayer, D.E. (1997).

Histone deacetylase activity is required for full transcriptional repression by mSin3A. Cell *89*, 341-347.

Henery, C.C., Miranda, M., Wiekowski, M., Wilmut, I., and DePamphilis, M.L. (1995). Repression of gene expression at the beginning of mouse development. Dev Biol *169*, 448-460.

Hill, K., Wang, H., and Perry, S.E. (2008). A transcriptional repression motif in the MADS factor AGL15 is involved in recruitment of histone deacetylase complex components. Plant J *53*, 172-185.

Ho, Y., Wigglesworth, K., Eppig, J.J., and Schultz, R.M. (1995). Preimplantation development of mouse embryos in KSOM: augmentation by amino acids and analysis of gene expression. Mol Reprod Dev *41*, 232-238.

Hoppe, P.C., and Pitts, S. (1973). Fertilization in vitro and development of mouse ova. Biol Reprod *8*, 420-426.

Howlett, S.K., and Bolton, V.N. (1985). Sequence and regulation of morphological and molecular events during the first cell cycle of mouse embryogenesis. J Embryol Exp Morph *87*, 175-206.

Howlett, S.K., and Reik, W. (1991). Methylation levels of maternal and paternal genomes during preimplantation development. Development *113*, 119-127.

Inoue, A., Matoba, S., and Zhang, Y. (2012). Transcriptional activation of transposable elements in mouse zygotes is independent of Tet3-mediated 5-methylcytosine oxidation. Cell Res *22*, 1640-1649.

Inoue, A., Shen, L., Dai, Q., He, C., and Zhang, Y. (2011). Generation and replication-dependent dilution of 5fC and 5caC during mouse preimplantation development. Cell Res *21*, 1670-1676.
Inoue, A., and Zhang, Y. (2011). Replication-dependent loss of 5-hydroxymethylcytosine in mouse preimplantation embryos. Science *334*, 194.

Iqbal, K., Jin, S.G., Pfeifer, G.P., and Szabo, P.E. (2011). Reprogramming of the paternal genome upon fertilization involves genome-wide oxidation of 5-methylcytosine. Proc Natl Acad Sci USA *108*, 3642-3647.

Ito, S., D'Alessio, A.C., Taranova, O.V., Hong, K., Sowers, L.C., and Zhang, Y. (2010). Role of Tet proteins in 5mC to 5hmC conversion, ES-cell self-renewal and inner cell mass specification. Nature *466*, 1129-1133.

Jin, Q., Yu, L.R., Wang, L., Zhang, Z., Kasper, L.H., Lee, J.E., Wang, C., Brindle, P.K., Dent, S.Y., and Ge, K. (2011). Distinct roles of GCN5/PCAF-mediated H3K9ac and CBP/p300-mediated H3K18/27ac in nuclear receptor

transactivation. EMBO J *30*, 249-262.

John, G.B., Gallardo, T.D., Shirley, L.J., and Castrillon, D.H. (2008). Foxo3 is a PI3K- dependent molecular switch controlling the initiation of oocyte growth. Dev Biol *321*, 197-204.

Johnson, J., Canning, J., Kaneko, T., Pru, J.K., and Tilly, J.L. (2004). Germline stem cells and follicular renewal in the postnatal mammalian ovary. Nature *428*, 145–150.

Johnson, K.D., and Bresnick, E.H. (2002). Dissecting long-range transcriptional mechanisms by chromatin immunoprecipitation. Methods *26*, 27-36.

Johnson, M.H., and Maro, B. (1986). Time and space in the mouse early embryo: a cell biological approach to cell diversification In Rossant, J., and Pedersen, R.A. (Eds), Experimental Approaches to Mammalian Embryonic Development. Cambridge Univ. Press, Cambridge, 35-65.

Kadamb, R., Mittal, S., Bansal, N., Batra, H., and Saluja, D. (2013). Sin3: Insight into its transcription regulatory functions. Eur J Cell Biol *92*, 237-246.

Kadosh, D., and Struhl, K. (1997). Repression by Ume6 involves recruitment of a complex containing Sin3 corepressor and Rpd3 histone deacetylase to target promoters. Cell *89*, 365-371.

Kezele, P., Nilsson, E., and Skinner, M.K. (2002). Cell-cell interactions in primordial follicle assembly and development. Front Biosci *7*, 1990-1996.

Kezele, P., Nilsson, E.E., and Skinner, M.K. (2005). Keratinocyte growth factor acts as a mesenchymal factor that promotes ovarian primordial to primary follicle transition. Biol Reprod *73*, 967-973.

Kim, J.M., Liu, H., Tazaki, M., Nagata, M., and Aoki, F. (2003). Changes in histone acetylation during mouse oocyte meiosis. J Cell Biol *162*, 37-46.

Knoepfler, P.S., and Eisenman, R.N. (1999). Sin meets NuRD and other tails of repression. Cell *99*, 447-450.

Kurasawa, S., Schultz, R.M., and Kopf, G.S. (1989). Egg-induced modifications of the zona pellucida of mouse eggs: effects of microinjected inositol 1,4,5-trisphosphate. Dev Biol *133*, 295-304.

Laemmli, U.K., and Quittner, S.F. (1974). Maturation of the head of bacteriophage T4. IV. The proteins of the core of the tubular polyheads and in vitro cleavage of the head proteins. Virology *62*, 483-499.

Lane, N., Dean, W., Erhardt, S., Hajkova, P., Surani, A., Walter, J. and Reik, W.

(2003). Resistance of IAPs to methylation reprogramming may provide a mechanism for epigenetic inheritance in the mouse. Genesis *35*, 88-93.

Larue, L., Ohsugi, M., Hirchenhain, J., and Kemler, R. (1994). E-cadherin null mutant embryos fail to form a trophectoderm epithelium. Proc Natl Acad Sci USA *91*, 8263-8267.

Latham, K.E., Solter, D., and Schultz, R.M. (1991). Activation of a two-cell stage-specific gene following transfer of heterologous nuclei into enucleated mouse embryos. Mol Reprod Dev *30*, 182-186.

Lehtonen, E. (1980). Changes in cell dimensions and intercellular contacts during cleavage-stage cell cycles in mouse embryonic cells. J Embryol Exp Morphol *58*, 231-249.

Lepikhov, K., and Walter, J. (2004). Differential dynamics of histone H3 methylation at positions K4 and K9 in the mouse zygote. BMC Dev Biol *4*, 12-16.

Liang, J., Wan, M., Zhang, Y., Gu, P., Xin, H., Jung, S.Y., Qin, J., Wong, J., Cooney, A.J., Liu, D. et al. (2008). Nanog and Oct4 associate with unique transcriptional repression complexes in embryonic stem cells. Nat Cell Biol *10*, 731-739.

Lin, C.J., Koh, F.M., Wong, P., Conti, M., and Ramalho-Santos, M. (2014). Hira-mediated H3.3 incorporation is required for DNA replication and ribosomal RNA transcription in the mouse zygote. Dev Cell *30*, 268-279.

Lin, T., Chao, C., Saito, S., Mazur, S.J., Murphy, M.E., Appella, E., and Xu, Y. (2005). p53 induces differentiation of mouse embryonic stem cells by suppressing Nanog expression. Nat Cell Biol *7*, 165-171.

Liu, H., and Aoki, F. (2002). Transcriptional activity associated with meiotic competence in fully grown mouse GV oocytes. Zygote *10*, 327-332.

Liu, H., Kim, J.M. and Aoki, F. (2004). Regulation of histone H3 lysine 9 methylation in oocytes and early pre-implantation embryos. Development *131*, 2269-2280.

Loppin, B., Bonnefoy, E., Anselme, C., Laurençon, A., Karr, T.L., and Couble, P. (2005). The histone H3.3 chaperone HIRA is essential for chromatin assembly in the male pronucleus. Nature *437*, 1386-1390.

Ma, J., Flemr, M., Strnad, H., Svoboda, P., and Schultz, R.M. (2013). Maternally recruited DCP1A and DCP2 contribute to messenger RNA degradation during oocyte maturation and genome activation in mouse. Biol Reprod *88*, 1-12.

Ma, P., DeWaal, E., Weaver, J.R., Bartolomei, M.S., and Schultz, R.M. (2015). A DNMT3A2-HDAC2 complex is essential for genomic imprinting and genome integrity in mouse oocytes. Cell Rep *13*, 1552-1560.

Ma, P., and Schultz, R.M. (2008). Histone deacetylase 1 (HDAC1) regulates histone acetylation, development, and gene expression in preimplantation mouse embryos. Dev Biol *319*, 110-120.

Ma, P., and Schultz, R.M. (2013). Histone deacetylase 2 (HDAC2) regulates chromosome segregation and kinetochore function via H4K16 deacetylation during oocyte maturation in mouse. PLoS Genet *9*, e1003377.

Ma, J., Svoboda, P., Schultz, R.M., and Stein, P. (2001). Regulation of zygotic gene activation in the preimplantation mouse embryo: Global activation and repression of gene expression. Biol Reprod *64*, 1713-1721.

Majumder, S., Miranda, M., and DePamphilis, M.L. (1993). Analysis of gene expression in mouse preimplantation embryos demonstrates that the primary role of enhancers is to relieve repression of promoters. EMBO J 12, 1131-1140.

Manejwala, F., Kaji, E., and Schultz, R.M. (1986). Development of activatable adenylate cyclase in the preimplantation mouse embryo and a role for cyclic AMP in blastocoel formation. Cell *46*, 95-103.

Mayer, W., Niveleau, A., Walter, J., Fundele, R., and Haaf, T. (2000). Demethylation of the zygotic paternal genome. Nature *403*, 501-502.

Medvedev, S., Yang, J., Hecht, N.B., and Schultz, R.M. (2008). CDC2A (CDK1)-mediated phosphorylation of MSY2 triggers maternal mRNA degradation during mouse oocyte maturation. Dev Biol *321*, 205-215.

Mi, H., Muruganujan, A., Casagrande, J.T., and Thomas, P.D. (2013). Large-scale gene function analysis with the PANTHER classification system. Nat Protoc *8,* 1551-1566.

Moore, G. P., and Lintern-Moore, S. (1978). Transcription of the mouse oocyte genome. Biol Reprod *18*, 865-870.

Murai, S., Stein, P., Buffone, M.G., Yamashita, S., and Schultz, R.M. (2010). Recruitment of Orc6l, a dormant maternal mRNA in mouse oocytes, is essential for DNA replication in 1-cell embryos. Dev Biol *341*, 205-212.

Nakamura, T., Liu, Y.J., Nakashima, H., Umehara, H., Inoue, K., Matoba, S., Tachibana, M., Ogura, A., Shinkai, Y., and Nakano, T. (2012). PGC7 binds histone H3K9me2 to protect against conversion of 5mC to 5hmC in early

embryos. Nature *486*, 415-419.

Nilsson, E.E., Detzel, C., and Skinner, M.K. (2006). Platelet-derived growth factor modulates the primordial to primary follicle transition. Reproduction *131*, 1007-1015.

Nilsson, E.E., and Skinner, M.K. (2004). Kit ligand and basic fibroblast growth factor interactions in the induction of ovarian primordial to primary follicle transition. Mol Cell Endocrinol *214*, 19-25.

Nonchev, S., and Tsanev, R. (1990). Protamine – histone replacement and DNA replication in the male mouse pronucleus. Mol Reprod Dev *25*, 72-76.

Nurse, P. (1990). Universal control mechanism regulating onset of M-phase. Nature *344*, 503-508.

Oh, B., Hwang, S., McLaughlin, J., Solter, D., and Knowles, B.B. (2000). Timely translation during the mouse oocyte-to-embryo transition. Development *127*, 3795-3803.

Oswald, J., Engemann, S., Lane, N., Mayer, W., Olek, A., Fundele, R., Dean, W., Reik, W. and Walter, J. (2000). Active demethylation of the paternal genome in the mouse zygote. Curr Biol *10*, 475-478.

Pacchiarotti, J., Maki, C., Ramos, T., Marh, J., Howerton, K., Wong, J., Pham, J., Anorve, S., Chow, Y.C., and Izadyar, F. (2010). Differentiation potential of germ line stem cells derived from the postnatal mouse ovary. Differentiation *79*, 159-170.

Palombella, V.J., Rando, O.J., Goldberg, A.L., and Maniatis, T. (1994). The ubiquitinproteasome pathway is required for processing the NF-kappa-B1 precursor protein and the activation of NF-kappa-B. Cell *78*, 773-785.

Park, S.J., Komata, M., Inoue, F., Yamada, K., Nakai, K., Ohsugi, M., and Shirahige, K. (2013). Inferring the choreography of parental genomes during fertilization from ultralarge-scale whole-transcriptome analysis. Genes Dev *27*, 2736-2748.

Peat, J.R., Dean, W., Clark, S.J., Krueger, F., Smallwood, S.A., Ficz, G., Kim, J.K., Marioni, J.C., Hore, T.A., and Reik, W. (2014). Genome-wide bisulfite sequencing in zygotes identifies demethylation targets and maps the contribution of TET3 oxidation. Cell Reports *9*, 1990-2000.

Pehrson J.R., and Fried, V.A. (1992). MacroH2A, a core histone containing a large nonhistone region. Science *257*, 1398-1400.

Ram, P.T. and Schultz, R.M. (1993). Reporter gene expression in G2 of the 1-cell mouse embryo. Dev Biol *156*, 552-556.

Reddy, P., Liu, L., Adhikari, D., Jagarlamudi, K., Rajareddy, S., Shen, Y., Du, C., Tang, W., Hamalainen, T., Peng, S.L., et al. (2008). Oocyte-specific deletion of Pten causes premature activation of the primordial follicle pool. Science *319*, 611-613.

Richter, J.D., and Sonenberg, N. (2005). Regulation of cap-dependent translation by eIF4E inhibitory proteins. Nature, *433*, 477-480.

Ritchie, M.E., Phipson, B., Wu, D., Hu, Y., Law, C.W., Shi, W., and Smyth, G.K. limma powers differential expression analyses for RNA-sequencing and micro-array studies. Nucleic Acids Res 2015; 43:e47.

Roest, H.P., Baarends, W.M., de Wit, J., van Klaveren, J.W., Wassenaar, E., Hoogerbrugge, J.W., van Cappellen, W.A., Hoeijmakers, J.H., and Grootegoed, J.A. (2004). The ubiquitin-conjugating DNA repair enzyme HR6A is a maternal factor essential for early embryonic development in mice. Mol Cell Biol *24*, 5485-5495.

Rougier, N., Bourc'his, D., Gomes, D.M., Niveleau, A., Plachot, M., Pa`ldi, A., and Viegas-Pequignot, E. (1998). Chromosome methylation patterns during mammalian preimplantation development. Genes Dev *12*, 2108-2113.

Russell, D.L., and Robker, R.L. (2007) Molecular mechanisms of ovulation: co-ordination through the cumulus complex. Hum Reprod Update 13, 289-312.

Sagata, N. (1997). What does Mos do in oocytes and somatic cells? Bioessays *19*, 13-21.

Santos, F., Hendrich, B., Reik, W., and Dean, W. (2002). Dynamic reprogramming of DNA methylation in the early mouse embryo. Dev Biol *241*, 172-182.

Santos, F., Peters, A.H., Otte, A.P., Reik, W. and Dean, D. (2005). Dynamic chromatin modifications characterise the first cell cycle in mouse embryos. Dev Biol *280*, 225-236.

Schroeder, A.C., and Eppig, J.J. (1984). The developmental capacity of mouse oocytes that matured spontaneously in vitro is normal. Dev Biol *102*, 493-497.

Schultz, R.M. (1993). Regulation of zygotic gene activation in the mouse. BioEssays *15*, 531-538.

Schultz, R.M., Montgomery, R.R., and Belanoff, J.R. (1983). Regulation of

mouse oocyte meiotic maturation: implication of a decrease in oocyte cAMP and protein dephosphorylation in commitment to resume meiosis. Dev Biol *97*, 264-273.

Skinner, M.K. (2005). Regulation of primordial follicle assembly and development. Hum Reprod Update *11*, 461-471.

Schindler, R., Nilsson, E., and Skinner, M.K. (2010). Induction of ovarian primordial follicle assembly by connective tissue growth factor CTGF. PLoS One *5*, e12979.

Sheets, M.D., Wu, M., and Wickens, M. (1995). Polyadenylation of *c-mos* mRNA as a control point in *Xenopus* meiotic maturation. Nature *374*, 511-516.

Shen, X., Liu, Y., Hsu, Y.J., Fujiwara, Y., Kim, J., Mao, X., et al. (2008). EZH1 mediates methylation on histone H3 lysine 27 and complements EZH2 in maintaining stem cell identity and executing pluripotency. Mol Cell *32*, 491-502.

Silverstein, R.A., and Ekwall, K. (2005). Sin3: a flexible regulator of global gene expression and genome stability. Curr Genet *47*, 1-17.

Smallwood, S.A., Tomizawa, S., Krueger, F., Ruf, N., Carli, N., Segonds-Pichon, A., Sato, S., Hata, K., Andrews, S.R., and Kelsey, G. (2011). Dynamic CpG island methylation landscape in oocytes and preimplantation embryos. Nature Genetics *43*, 811-814.

Smith, K.T., Sardiu, M.E., Martin-Brown, S.A., Seidel, C., Mushegian, A., Egidy, R., et al. (2012). Human family with sequence similarity 60 member A (FAM60A) protein: A new subunit of the Sin3 deacetylase complex. Mol Cell Proteomics *11*, 1815-1828.

Sorensen, R.A., and Wassarman, P.M. (1976). Relationship between growth and meiotic maturation of the mouse oocyte. Dev Biol *50*, 531-536.

Stebbins-Boaz, B., Cao, Q., de Moor, C.H., Mendez, R., and Richter, J.D. (1999). Maskin is a CPEB-associated factor that transiently interacts with eIF-4E. Mol Cell *4*, 1017-1027.

Su, Y.Q., Sugiura, K., Woo, Y., Wigglesworth, K., Kamdar, S., Affourtit, J., and Eppig, J.J. (2007). Selective degradation of transcripts during meiotic maturation of mouse oocytes. Dev Biol *302*, 10 Richter 4-117.

Szybek, K. (1972). In vitro maturation of oocytes from sexually immature mice. J Endocrinol *54*, 527-528.

Tachibana, M., Sugimoto, K., Nozaki, M., Ueda, J., Ohta, T., Ohki, M., Fukuda, M., Takeda, N., Niida, H., Kato, H. et al. (2002). G9a histone methyltransferase

plays a dominant role in euchromatic histone H3 lysine 9 methylation and is essential for early embryogenesis. Genes Dev *16*, 1779-1791.

Tahiliani, M., Koh, K.P., Shen, Y., Pastor, W.A., Bandukwala, H., Brudno, Y., Agarwal, S., Iyer, L.M., Liu, D.R., Aravind, L., Rao, A. (2009). Conversion of 5-methylcytosine to 5-hydroxymethylcytosine in mammalian DNA by MLL partner TET1. Science *324*, 930-935.

Tateno, H., and Kamiguchi, Y. (2007). Evaluation of chromosomal risk following intracytoplasmic sperm injection in the mouse. Biol Reprod *77*, 336-342.

Tong, Z.B., Gold, L., Pfeifer, K.E., Dorward, H., Lee, E., Bondy, C.A., Dean, J., and Nelson, L.M. (2000). Mater, a maternal effect gene required for early embryonic development in mice. Nat Genet *26*, 267-268.

Torres-Padilla, M.E., and Zernicka-Goetz, M. (2006). Role of TIF1alpha as a modulator of embryonic transcription in the mouse zygote. J Cell Biol *174*, 329-338.

Touitou, R., Richardson, J., Bose, S., Nakanishi, M., Rivett, J., and Allday, M.J. (2001). A degradation signal located in the C-terminus of p21WAF1/CIP1 is a binding site for the C8 alpha-subunit of the 20S proteasome. EMBO J *20*, 2367-2375.

Toyoda, Y., Yokoyama, M., and Hosi, T. (1971). Studies on the fertilization of mouse eggs in vitro: I. in vitro fertilization of eggs by fresh epididymal sperm. Jpn J Anim Reprod *16*, 147-151.

Tsafriri, A., Chun, S.Y., Zhang, R., Hsueh, A.J., and Conti, M. (1996). Oocyte maturation involves compartmentalization and opposing changes of cAMP levels in follicular somatic and germ cells: studies using selective phosphodiesterase inhibitors. Dev Biol *178*, 393-402.

Verlhac, M.H., Pennart, H.D., Maro, B., Cobb, M.H., and Clarke H.J. (1993). MAP kinase becomes stably activated at metaphase and in associated with microtubule-organizing centers during meiotic maturation of mouse oocytes. Dev Biol *158*, 330-340.

Verreault, A., Kaufman, P.D., Kobayashi, R., and Stillman, B. (1998). Nucleosomal DNA regulates the core-histone-binding subunit of the human Hat1 acetyltransferase. Curr Biol *8*, 96-108.

Wang, H., Cao, R., Xia, L., Erdjument-Bromage, H., Borchers, C., Tempst, P., and Zhang, Y. (2001). Purification and functional characterization of a histone H3-lysine 4-specific methyltransferase. Mol Cell *8*, 1207-1217.

Wang, Z., Zang, C., Rosenfeld, J.A., Schones, D.E., Barski, A., Cuddapah, S., Cui, K., Roh, T.Y., Peng, W., Zhang, M.Q., and Zhao, K. (2008). Combinatorial patterns of histone acetylations and methylations in the human genome. Nat Genet *40*, 897-903.

Wei, H., Wang, Q., Du, J., Li, X., Zhang, N., Cao, Y., and Ma, W. (2015). Unique subcellular distribution of RPB1 with a phosphorylated C-terminal domain (CTD) in mouse oocytes during meiotic division and its relationship with chromosome separation. J Reprod Dev *61*, 541-548.

White, Y.A.R., Woods, D.C., Takai, Y., Ishihara, O., Seki, H., and Tilly, J.L. (2012). Oocyte formation by mitotically active germ cells purified from ovaries of reproductive-age women. Nat Med *18*, 413-421.

Wickramasinghe, D., Ebert, K.M., and Albertini, D.F. (1991). Meiotic competence acquisition is associated with the appearance of M-phase characteristics in growing mouse oocytes. Dev Biol *143*, 162-172.

Wiekowski, M., Miranda, M., and DePamphilis, M.L. (1991). Regulation of gene expression in preimplantation mouse embryos: effects of the zygotic clock and the first mitosis on promoter and enhancer activities. Dev Biol 147, 403-414.

Wiekowski, M., Miranda, M., and DePamphilis, M.L. (1993). Requirements for promoter activity in mouse oocytes and embryos distinguish paternal pronuclei from maternal and zygotic nuclei. Dev Biol *159*, 366-378.

Worrad, D.M., Ram, P.T., and Schultz, R.M. (1994). Regulation of gene expression in the mouse oocyte and early preimplantation embryo: developmental changes in Sp1 and TATA box-binding protein, TBP. Development *120*, 2347-2357.

Wossidlo, M., Nakamura, T., Lepikhov, K., Marques, C.J., Zakhartchenko, V., Boiani, M., Arand, J., Nakano, T., Reik, W., and Walter, J. (2011). 5-Hydroxymethylcytosine in the mammalian zygote is linked with epigenetic reprogramming. Nat Commun *241*, 1-8.

Yang, L. Mei, Q., Zielinska-Kwiatkowska, A., Matsui, Y., Blackburn, M.L., Benedetti, D., Krumm, A.A., Taborsky, G.J. Jr., Chansky, H.A. (2003). An ERG (ets-related gene)-associated histone methyltransferase interacts with histone deacetylases 1/2 and transcription co-repressors mSin3A/ B. Biochem J *369*, 651-657.

Yoshida, M., Horinouchi, S., and Beppu, T. (1995). Trichostatin A and trapoxin: novel chemical probes for the role of histone acetylation in chromatin structure and function. BioEssays *17*, 423-430.

You, A., Tong, J.K., Grozinger, C.M., and Schreiber, S.L. (2001). CoREST is an integral component of the CoREST- human histone deacetylase complex. Proc Natl Acad Sci USA *98*, 1454-1458.

Yu, J., Deng, M., Medvedev, S., Yang, J., Hecht, N.B., and Schultz, R.M. (2004). Transgenic RNAi-mediated reduction of MSY2 in mouse oocytes results in reduced fertility. Dev Biol *268*, 195-206.

Zeng, F., Baldwin, D.A., and Schultz, R. (2004). Transcript profiling during preimplantation mouse development. Dev Biol *272*, 483-496.

Zeng, F., and Schultz, R.M. (2005). RNA transcript profiling during zygotic gene activation in the preimplantation mouse embryo. Dev Biol *283*, 40-57.

Zhang, Y., Ng, H.H., Erdjument-Bromage, H., Tempst, P., Bird, A., and Reinberg, D. (1999). Analysis of the NuRD subunits reveals a histone deacetylase core complex and a connection with DNA methylation. Genes Dev *13*, 1924-1935.

Zou, K., Yuan, Z., Yang, Z., Luo, H., Sun, K., Zhou, L., Xiang, J., Shi, L., Yu, Q., Zhang, Y., et al. (2009). Production of offspring from a germline stem cell line derived from neonatal ovaries. Nat Cell Biol *11*, 631-636.

Zuckerman, S. (1951). The number of oocytes in the mature ovary. Recent Prog Horm Res *6*, 63-108.